

THE UNIVERSITY OF CALGARY

Synaptic Signalling in the Outer Plexiform
Layer of the Vertebrate Retina.

by

Vaishali Merchant

A THESIS SUBMITTED TO THE FACULTY OF GRADUATE STUDIES IN
PARTIAL FULFILLMENT OF THE REQUIREMENTS FOR THE
DEGREE OF MASTER OF SCIENCE

DEPARTMENT OF NEUROSCIENCES

CALGARY, ALBERTA

JANUARY, 1993

© Vaishali Merchant 1993



National Library
of Canada

Bibliothèque nationale
du Canada

Acquisitions and
Bibliographic Services Branch

Direction des acquisitions et
des services bibliographiques

395 Wellington Street
Ottawa, Ontario
K1A 0N4

395, rue Wellington
Ottawa (Ontario)
K1A 0N4

Your file *Votre référence*

Our file *Notre référence*

The author has granted an irrevocable non-exclusive licence allowing the National Library of Canada to reproduce, loan, distribute or sell copies of his/her thesis by any means and in any form or format, making this thesis available to interested persons.

L'auteur a accordé une licence irrévocable et non exclusive permettant à la Bibliothèque nationale du Canada de reproduire, prêter, distribuer ou vendre des copies de sa thèse de quelque manière et sous quelque forme que ce soit pour mettre des exemplaires de cette thèse à la disposition des personnes intéressées.

The author retains ownership of the copyright in his/her thesis. Neither the thesis nor substantial extracts from it may be printed or otherwise reproduced without his/her permission.

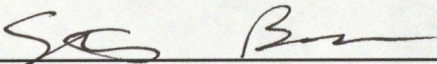
L'auteur conserve la propriété du droit d'auteur qui protège sa thèse. Ni la thèse ni des extraits substantiels de celle-ci ne doivent être imprimés ou autrement reproduits sans son autorisation.

ISBN 0-315-83214-2

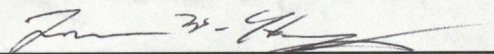
Canada

THE UNIVERSITY OF CALGARY
FACULTY OF GRADUATE STUDIES

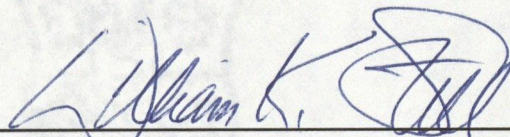
The undersigned certify that they have read, and recommend to the Faculty of Graduate Studies for acceptance, a thesis entitled, "Synaptic Signalling in the Outer Plexiform Layer of the Vertebrate Retina" submitted by Vaishali Merchant in partial fulfillment of the requirements for the degree of Master of Science.



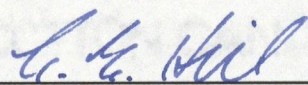
Supervisor, Steven Barnes
Department of Medical Physiology



Lawrence W. Haynes
Department of Medical Physiology



William K. Stell
Department of Anatomy



External, Ceredwyn E. Hill
Department of Biological Sciences

Date 4 January 1993

Abstract

Input-output relations between photoreceptors and second order cells in the outer plexiform layer of the larval tiger salamander (*Ambystoma tigrinum*) retina were studied by analyzing the cone photoreceptor output synapse and synaptic feedback to cones. The retinal slice preparation facilitated the identification of cells. The effects of extracellular pH (pH_O) on synaptic transmission were studied by recording whole-cell postsynaptic currents in different pH_O 's. Light-elicited postsynaptic currents were exponentially dependent on pH_O , exhibiting an e-fold increase in current per 0.23 pH unit in the range of pH 7 to 8. This action was probably via modulation of presynaptic photoreceptor Ca channels. Involvement of the proposed GABA_A receptor/chloride channel in feedback to cones was also investigated. The reversal potential of the feedback response was extrapolated to be 0 mV. GABA irreversibly reduced calcium-activated currents. These pre- and postsynaptic mechanisms are discussed in relation to synaptic transmission generally in the nervous system.

Acknowledgments

I would sincerely like to thank my supervisor, Dr. S. Barnes, for being a mentor, role model, and friend. Thank you for your patience during the learning stage, encouragement during the low periods, and enthusiasm during the high points. Your open door policy was greatly appreciated.

I also wish to thank Dr. W. K. Stell and Dr. L.W. Haynes for their time and effort in advising me when I needed help.

Throughout my time as a graduate student I was fortunate to befriend many fellow students who made it easier for me to recognize that student life could be serious, fun, logical, insane, and sometimes silly. Aside from those whose names I couldn't include, I would especially like to thank Nadine Ewadinger, Doug Fraser, Farid Mahmud, Gerald Zamponi, Janice Braun, Paul van Donkelaar, and Scott Day.

I thank my friends Erane van Blommestein and Kerri Schmidt for their devotion and constant support.

Last, but not least, I would like to thank my family, Mom, Dad, and Kris, for their confidence and faith that I was doing the right thing. I accomplished this work because of your belief.

Table of Contents

Title Page	i
Approval Page	ii
Abstract	iii
Acknowledgements	iv
Table of Contents	v
List of Figures	vii
1 Introduction	1
1.1 Lateral interactions at the OPL	1
1.2 Morphology	3
1.3 The photoreceptor output synapse	5
1.3.1 The photoreceptor response to light	5
1.3.2 Postsynaptic receptors.	5
1.3.3 Mechanism of synaptic transfer	6
1.3.4 pH	7
1.3.5 Goals of the study	8
1.4 Synaptic inputs to cones	9
1.4.1 Feed-forward pathway	9
1.4.2 Feedback pathway.	9
1.4.3 Mechanism of GABA mediated feedback	10
1.4.4 Goals of the study	11
2 Materials and Methods	12
2.1 Retinal slice preparation.	12
2.2 Solutions	13
2.3 Whole-cell patch-clamp recording and analysis	13
2.4 Light stimulation	14
2.5 Computer modelling	15
3 Results	17
3.1 Properties of cones	17
3.1.1 Morphology and simulation of transmission within cones	17
3.1.1.1 Morphological and passive electrical parameters	17
3.1.1.2 Computer modelling of communication within a cone.	24
3.1.1.3 Conclusion	29
3.1.2 Ionic currents in the inner segment of cones.	29
3.1.2.1 I_{Ca} , I_{Ca} -activated currents, and pH	29
3.1.2.2 I_K	37
3.1.2.3 I_h and I_{Kx}	37
3.1.2.4 Conclusion	38
3.1.3 The cone light response	41
3.1.3.1 Log light intensity versus current	41
3.1.3.2 Wavelength dependence.	41
3.1.3.3 Conclusion	48

3.2 Feedforward transmission	49
3.2.1 Light-elicited currents of second order cells	49
3.2.1.1 Horizontal cells and OFF-bipolar cells	49
3.2.1.2 ON-bipolar cells	52
3.2.1.3 Conclusion	59
3.2.2 pH modulation of synaptic transmission	59
3.2.2.1 Exponential dependence of postsynaptic currents on pH_O	59
3.2.2.2 Shifts of the synaptic transfer function	64
3.2.2.3 Conclusion	69
3.3 Feedback to cones	70
3.3.1 Methods of generating the feedback signal	70
3.3.1.1 The headless cone	70
3.3.1.2 Driving the rod network using TEA.	71
3.3.1.3 Pumping up the horizontal cell	71
3.3.1.4 Conclusion	72
3.3.2 The feedback response	72
3.3.2.1 Reversal potential of the feedback response	75
3.3.2.2 Modulation of ion channels	78
3.3.2.3 Conclusion	83
4 Discussion	84
4.1 The cone photoreceptor	84
4.1.1 Coupling between the cell body and telodendrite is good bidirectionally	84
4.1.2 Ionic currents of the inner segment shape the responses of cones	85
4.1.3 Cones respond maximally to bright light of 600 to 650 nm	86
4.2 pH_O and synaptic transmission	88
4.2.1 Postsynaptic cells are modulated by changes of pH_O	88
4.2.2 Modulation of presynaptic Ca channels account for the exponential dependence of postsynaptic currents on pH_O	88
4.2.3 Activity dependent pH changes are widespread in the nervous system	90
4.2.4 Relevance to synaptic gain	90
4.3 Mechanisms of feedback.	92
4.3.1 The feedback response reversal potential varies	92
4.3.2 GABA may modulate calcium-activated currents	93
4.4 Function of the OPL	95
4.4.1 Contrast enhancement	95
4.4.2 Outputs and inputs in the OPL	96
References	97

List of Figures

1	Photograph of a larval tiger salamander retinal slice	18
2	Lucifer yellow fill of a cone photoreceptor.	20
3	Morphological and passive electrical properties of cones.	22
4	Simulation of a synaptic input at a $1\ \mu\text{m}$ diameter telodendrite during a 30 pA light response.	26
5	Barium currents of cones	30
6	Modulation of barium current by changes of extracellular pH	33
7	Whole-cell currents showing I_K , $I_{K(Ca)}$, and $I_{Cl(Ca)}$	35
8	I_h and I_{KX} in a voltage-clamped cone	39
9	Photocurrent of one member of a dark-adapted double cone	42
10	Photocurrents of a dark-adapted single cone at varying intensities of light	44
11	Cone light responses as a function of wavelength of light	46
12	Whole-cell and light-elicited properties of a horizontal cell	50
13	Light-elicited horizontal cell currents at varying intensities of light	53
14	Whole-cell and light-elicited properties of an ON-bipolar cell	55
15	Light-elicited ON-bipolar cell currents at varying intensities of light	57
16	Modulation of postsynaptic horizontal cell currents by changes of extracellular pH	60
17	Exponential dependence of postsynaptic current on extracellular pH	62
18	Modulation of postsynaptic ON-bipolar cell currents by changes of extracellular pH	65
19	Lateral shifts of the synaptic transfer function	67
20	Generation and resolution of the feedback signal in cones	73
21	Reversal potential of the feedback response in a headless cone	76
22	Modulation of $I_{K(Ca)}$ in a cone by $100\ \mu\text{M}$ GABA	79
23	Modulation of $I_{Cl(Ca)}$ in a cone by $100\ \mu\text{M}$ GABA	81

CHAPTER 1

INTRODUCTION

The outer plexiform layer (OPL) of the vertebrate retina is the first stage of signal processing in the visual system. Cells synapsing in this layer generate basic phenomena that are important for vision. The variety of cells interacting in this layer include the light-sensitive photoreceptors (rods and cones), second-order horizontal cells and bipolar cells, and interplexiform cells.

1.1 Lateral Interactions In The Outer Plexiform Layer

Early recordings from ganglion cells of the cat retina showed that these cells have center-surround antagonistic receptive fields (Kuffler, 1953). Similar center-surround antagonistic receptive fields were found at the level of bipolar cells in the mudpuppy retina (Werblin & Dowling, 1969). Center-surround antagonism originates at the level of the OPL where interactions occur between the photoreceptors, horizontal cells, and bipolar cells.

A receptive field is defined for the visual system as a limited area of visual space over which a cell can detect a stimulus (Kuffler, Nicholls, & Martin, 1984, p. 19). A center-surround antagonistic receptive field is defined as a receptive field having two concentric regions in which responses are antagonistic to each other (Kuffler, 1953). Response to stimulation in a central region or area is antagonized by response to stimulation in the surrounding area.

There are several varieties of center-surround antagonistic receptive fields. One of the simplest types in the vertebrate retina is the bipolar cell receptive field wherein cell excitation with central illumination is inhibited by surround illumination (i.e. depolarization of an ON-bipolar cell (center-depolarizing) with central illumination and hyperpolarization with surround illumination or

hyperpolarization of an OFF-bipolar cell (center-hyperpolarizing) with central illumination and depolarization with surround illumination). Functionally, this type of lateral inhibition gives rise to contrast enhancement or edge detection, which is revealed by so called Mach Bands (brighter regions) at either side of a region of sharply changing contrast.

How does this mechanism enhance contrast or detect edges? First of all, consider broad field illumination (i.e. no edges) falling on a perfectly concentric center-surround antagonistic receptive field. Central and surround cones are stimulated equally and the entire bipolar cell receptive field is stimulated. Lateral inhibition essentially cancels central and surround responses and the bipolar cell responds minimally. An edge (a light and dark area) that cuts through exactly one half of the bipolar cell receptive field will also produce a minimal response in the bipolar cell. Once again, responses of cones in one half of the bipolar cell receptive field are cancelled out by lateral inhibitory responses of cones in the other half of the bipolar cell antagonistic surround. However, an edge transecting more than half of the bipolar cell receptive field will produce a greater response in the bipolar cell. Responses of cones in the central region of the bipolar cell receptive field will outweigh responses of cones in the antagonistic surround region. The bipolar cell response will be greater because of unbalanced weighting of responses in central and surround regions and this comprises an "edge" signal that will be transmitted to proximal levels of the retina and to the central nervous system.

Center-surround antagonistic receptive fields originate in the OPL in bipolar cells and form the basis of ON and OFF pathways of vision. The OPL serves to enhance responses to contrasting stimuli. Two important components of OPL function can be analyzed: the operation of the photoreceptor output synapse and

synaptic inputs to cones from horizontal cells. Attwell, Werblin, Wilson, and Wu (1983) showed that rods do not receive synaptic inputs from horizontal cells in tiger salamander retina. Simultaneous microelectrode recordings showed that current injected into a rod was recorded as voltage from a nearby cone, probably due to feedback connections between horizontal cells and cones. Coupling via gap junctions between rods and cones is low (Attwell, Wilson, & Wu, 1984) and probably does not account for these results. Furthermore, current injected into a cone was not recorded in a nearby rod suggesting a lack of synaptic input from horizontal cells to rods (Attwell *et al.*, 1983).

1.2 Morphology

The photoreceptor cells of the salamander retina are single and double cones, red rods, and green rods (Walls, 1942; Attwell, Wilson, & Wu, 1984). Photoreceptors make several types of junctions that can be observed under electron microscopy, including ribbon, basal, and distal junctions. Ribbon junctions are characterized by an electron-dense ribbon or lamella that is oriented at right angles to the presynaptic membrane (Dowling, 1987, p. 48). Basal junctions link the basal surface of photoreceptor pedicles to hundreds of fine cell processes (Lasansky, 1969). Generally, a bipolar cell process in the center of a triad of an invaginating ribbon synapse is flanked by two horizontal cells processes (the lateral processes). Distal junctions occur when one or more visual cell processes abut upon the lateral processes in a triad (Lasansky, 1971).

Photoreceptors make invaginating ribbon synapses with several bipolar cells and horizontal cells in the OPL of most non-mammalian vertebrates (Lasansky, 1971, 1973; Dowling & Werblin, 1969). Basal junctions in non-mammalian vertebrates are usually made by cones and rods while in mammals mostly cones

make basal junctions (Dowling, 1987, p. 49). It was found that center-hyperpolarizing bipolar cells (Werblin & Dowling, 1969) made mainly ribbon junctions and center-depolarizing bipolar cells made mainly basal junctions in tiger salamander retina (Lasansky, 1978). However, both bipolar cell types also made all of the possible varieties of contacts with rods and cones.

Horizontal cell bodies make ribbon and distal junctions with rods and cones (Lasansky, 1978). Goldfish horizontal cells are classified into four types and form colour specific interconnections (Stell & Lightfoot, 1975). Evidence has shown that synapses are present between horizontal cells and bipolar cells in cold-blooded vertebrates including amphibians (Dowling, 1968; Dowling and Werblin, 1969; Lasansky, 1973), reptiles (Kolb and Jones, 1984), and fishes (Sakai and Naka, 1986; Marshak and Dowling, 1987).

Gap junctions are present between photoreceptors and between horizontal cells. In tiger salamander retina, rods are strongly coupled to each other while the small cone to cone coupling is thought to be via intervening rods (Attwell, Wilson, & Wu, 1984). Wu and Yang (1988) found that a hybrid rod called rod_c existed in salamander retina that had both rod and cone responses in the dark and only cone responses with background illumination. It is thought that these rods were more strongly coupled to cones than other rods and underwent a Purkinje shift (from 520 nm to 620 nm). Turtle double cones have been shown to make gap junctions with each other via basal processes or telodendria (Kolb & Jones, 1984).

A large variety of specific connections that mediate interactions between cells are formed in the OPL. This layer can be considered as a simplified network in the central nervous system in which general properties of cell to cell interaction can be analyzed and applied to larger networks and regions.

1.3 The Photoreceptor Output Synapse

1.3.1 The Photoreceptor Response to Light

Signals in the outer retina are graded. In the dark, a standing inward current (or dark current) maintains the membrane potential of photoreceptors near -40 mV. Many years of biochemical and electrophysiological effort (for review see Matthews & Baylor, 1981; Stryer, Hurley, & Fung, 1981; Liebman, & Pugh, Jr., 1981; Bitensky, Wheeler, Yamazaki, Rasenick & Stein, 1981; Miller, 1981; Stryer, 1986) have shown that when light falls upon a rod and is absorbed by rhodopsin, enzymes are activated that result in the closure of cyclic guanosine monophosphate (cGMP) - gated channels in the outer segment (Fesenko, Kolesnikov, & Lyuborsky, 1985; Nakatani & Yau, 1985; Haynes & Yau, 1985). Closure of these sodium (Na)- and calcium (Ca) -permeable channels hyperpolarizes the rod. While the amount of hyperpolarization is dependent upon the intensity of light, the maximum change in potential is about 20 mV. A similar mechanism of transduction is present in cones. Photoreceptor hyperpolarization induced by light results in a decrease of transmitter release, signalling detection of light to bipolar cells and horizontal cells. This signal is then transmitted to proximal levels of the retina and to the central nervous system.

1.3.2 Postsynaptic Receptors

Central regions of center-surround antagonistic receptive fields in bipolar cells are formed through direct synaptic inputs from the photoreceptors. Glutamate, the photoreceptor transmitter (Murakami, Ohtsu, & Ohtsuka, 1972; Dowling & Ripps, 1972; Cervetto & MacNichol, Jr., 1972; Wu & Dowling, 1978; Ishida & Fain, 1981; Lasater & Dowling, 1982), acts at non-*N*-methyl-*D*-aspartic acid (NMDA) post-synaptic receptors of bipolar cells and horizontal cells. Depolarizing bipolar cells (ON-bipolar cells) are the only cells in the vertebrate

central nervous system that are known to be hyperpolarized by glutamate. Whole-cell patch-clamp recordings from depolarizing bipolar cells in larval tiger salamander retinal slices have shown that glutamate acts at 2-amino-4-phosphonobutyric acid (APB) receptors and suppresses a cGMP-activated conductance (Nawy & Jahr, 1990, 1991) similar but not identical (Shiells & Falk, 1992b) to the cGMP conductance in the outer segments of photoreceptors. The gating of these cGMP-dependent channels is not thought to be mediated by protein kinases and does not require phosphorylation (Shiells & Falk, 1992a).

Horizontal cells and hyperpolarizing bipolar cells (OFF-bipolar cells) are depolarized by glutamate. Intracellular recordings of horizontal cells in salamander retina have shown the co-existence of kainate receptors, AMPA (α -amino-3-hydroxy-5-methyl-4-isoxalone propionic acid) receptors, and CNQX (6-cyano-7-nitroquinoxaline-2,3-dione)-resistant quisqualate receptors (Yang & Wu, 1991). Isolated OFF-bipolar cells from the salamander retina showed a conductance increase in the presence of kainate and quisqualate (Wilson, Gleason, & Gilbertson, 1991) while NMDA had no effect on these cells. It is thought that horizontal cells and hyperpolarizing bipolar cells probably use similar types of glutamate receptors (Slaughter & Miller, 1981, 1983a, 1985).

1.3.3 Mechanism Of Synaptic Transfer In The Retina

Photoreceptors are depolarized in the dark and are continuously releasing their neurotransmitter, glutamate. Glutamate acting at postsynaptic receptors maintains horizontal cells and hyperpolarizing bipolar cells at a depolarized potential (around -40 mV) and depolarizing bipolar cells at a negative potential (around -60 mV). Light hyperpolarizes the photoreceptor and consequently hyperpolarizes horizontal cells and OFF-bipolar cells and depolarizes ON-bipolar cells. As a result, the ON and OFF channels of the visual system are generated.

Much research has been focused on the reliability of transmission from the photoreceptors to their second order cells. Intracellular microelectrode recordings of turtle bipolar cells revealed that the synaptic transfer is 5 to 10 times faster from cones to hyperpolarizing bipolar cells than from cones to depolarizing bipolar cells and synaptic transfer from rods to horizontal cells is almost ten times slower than that from cones to the same horizontal cells (Copenhagen, Ashmore, & Schnapf, 1983). The gain of synaptic transmission from a turtle red cone to a horizontal cell is highest for small hyperpolarizing responses in the cone, in the range of 1 to 12 mV (Lasater & Witkovsky, 1991). At the rod output synapse only potential changes within 5 mV of the rod dark potential are transmitted faithfully to postsynaptic horizontal cells in the tiger salamander retina (Attwell, Borges, Wu, & Wilson, 1987). The variance in the rate of synaptic transfer between photoreceptors and different types of second order cells probably reflects differences in presynaptic transmission properties and postsynaptic receptor mechanisms. These results suggest that synaptic transfer from photoreceptors to second order cells is reliable with small hyperpolarizations of the photoreceptors. With such a reliable and sensitive system, it is possible that neuromodulators could shape the properties of the photoreceptor output synapse and possibly change its transfer characteristics. One such neuromodulator is extracellular pH.

1.3.4 pH

There is a widely held notion that interstitial pH is very tightly regulated. However, Chesler (1990) compiled data from various tissues and showed that activity dependent pH change are widespread in the nervous system. For example, in the drone bee retina, light stimulation produces alkaline shifts of greater than two tenths of a pH unit within one minute. Other work has shown that significant light induced pH_O shifts occur in cat, frog, and with prolonged illumination, toad

retina (Yamamoto, Borgula, & Steinberg, 1992; Borgula, Karwoski, & Steinberg, 1989; Oakley II, & Wen, 1989).

Previous work in the tiger salamander retina has shown that changes of pH_O modulate calcium channels of cones (Barnes & Bui, 1991) and rods (Mahmud & Barnes, 1992). In brief, changes to alkaline pH_O shift the Ca channel activation curve negatively along the voltage axis while changes to acidic pH_O shift activation positively along the voltage axis.

1.3.5 Goals Of The Study

Calcium channels play an important role in synaptic transmission. It is possible that modulation of presynaptic calcium channels by extracellular pH would affect synaptic transmission. Intracellularly recorded light responses of horizontal cells in salamander retina have been shown to be sensitive to pH_O (Kleinschmidt, 1991). It is important to determine whether synaptic transmission from photoreceptors to horizontal cells and bipolar cells in the retina can be modulated by changes of pH_O . The whole-cell patch-clamp will be used to facilitate the analysis of the pre- and postsynaptic ion channels that may be involved. The retinal slice technique will aid in the identification of postsynaptic horizontal cells and bipolar cells. Broad field illumination should generate postsynaptic currents that are relatively large and stable. If activity dependent pH changes are present through out the nervous system, then modulation of presynaptic calcium channels and consequently synaptic transmission may be a novel mechanism of synaptic regulation in the nervous system.

1.4 Synaptic Inputs To Cones

1.4.1 Feed-forward Pathway

Lateral interactions in the OPL of the vertebrate retina generate the center-surround antagonistic receptive fields of bipolar cells (Werblin & Dowling, 1969) and are mediated, at least in part, by horizontal cell feedback to cone photoreceptors (Baylor, Fourtes, & O'Bryan, 1971). Horizontal cells with large receptive fields mediate lateral interactions between photoreceptors and between photoreceptors and bipolar cells. Several mechanisms for lateral signal integration have been proposed. One mechanism for which anatomical evidence exists (Dowling, 1968; Dowling and Werblin, 1969; Lasansky, 1973; Kolb and Jones, 1984; Sakai and Naka, 1986; Marshak and Dowling, 1987) involves a feed-forward pathway from horizontal cells to bipolar cells. Here, illumination of cones in the surround of the bipolar cell receptive field hyperpolarizes horizontal cells which then feed forward onto bipolar cells.

1.4.2 Feedback Pathway

Another mechanism of lateral signal integration for which electrophysiological evidence exists involves a feedback pathway from horizontal cells to cones (Baylor, Fuortes, & O'Bryan, 1971; Attwell *et al.*, 1983; Skryzpek & Werblin, 1983). Illumination of the surround of the bipolar cell receptive field drives hundreds of cone photoreceptors and subsequently drives horizontal cells that feed back onto the cones in the center of the bipolar cell receptive field.

This feedback pathway may be due to a sign-inverting chemical synapse (Attwell *et al.*, 1983) and may involve the release of γ -aminobutyric acid (GABA) from horizontal cells onto cone photoreceptors (Marc, Stell, Bok, & Lam, 1978; Ayoub and Lam, 1984; Yazulla, 1985). [^3H] GABA was shown to be released by goldfish H1 horizontal cells (Marc *et al.*, 1978; Ayoub & Lam, 1984) during

dark-induced depolarizations and during superfusion of L-glutamate and L-aspartate (Yazulla, 1985). In salamander retina approximately 25% of horizontal cells showed [³H] GABA uptake (Wu, 1986). Furthermore, whole-cell patch-clamp recordings of isolated cones in turtle retina have shown that this feedback signal may act via GABA_A receptor/chloride (Cl) channels (Kaneko & Tachibana, 1986).

Attwell *et al.* (1983), Skrzypek and Werblin (1983) and Wu (1991) recorded a reversal potential of the feedback response of -65 mV (close to the chloride equilibrium potential) in tiger salamander cones. In contrast to these findings, Thoreson and Burkhardt (1990) have evidence from microelectrode recordings of turtle cones in eyecups and retinal slices suggesting that GABAergic mechanisms may not be involved at all in the feedback response. They showed that superfusion of GABA_A and GABA_B receptor agonists and antagonists onto the retina had no effect on the annulus induced graded depolarization thought to be the feedback response. Species differences may account for these findings. Furthermore, another mechanism of feedback not dependent on a chemical feedback synapse but on electric field intensity in the photoreceptor-horizontal cell extracellular gap has also been proposed (Byzov, Golubtsov, & Trifonov, 1977; Byzov & Shura-Bura, 1986).

1.4.3 Mechanism Of GABA Mediated Feedback

In the dark, cones and horizontal cells rest at a relatively depolarized level and both tonically release their respective transmitters, glutamate and (putatively) GABA. A spot of light in the center of the bipolar cell receptive field hyperpolarizes the central cones but only slightly hyperpolarizes the horizontal cells. There will be a large reduction of glutamate release from central cones but only a slight reduction of GABA release from horizontal cells. A spot plus a surround stimulus hyperpolarizes central and surround cones and strongly

hyperpolarizes horizontal cells. A substantial decrease of GABA release from horizontal cells onto central cones will result in the closure of the GABA_A receptor/Cl channels, chloride conductance will decrease in the central cones and they will depolarize. For these cones to depolarize, one must assume that the chloride equilibrium potential is more negative than the dark potential of about -40 mV. Depolarization of the central cones caused by surround illumination opposes (or inhibits) the hyperpolarization induced by the spot of light on these cones.

1.4.4 Goals Of The Study

The purpose of the research will be to characterize the feedback synapse by exploiting the retinal slice technique in which access to photoreceptors for recording is very good compared to that in wholemount and eyecup preparations. In addition, diffusional barriers to exogenously applied pharmacological agents are minimized for cells at the surface of the slice. It is important to determine whether the feedback response, already recorded in whole-mount and slice preparations using microelectrodes (Attwell *et al.*, 1983), can be recorded from cones in retinal slices using patch electrodes. Furthermore, if the feedback response originates in the telodendria of cones, it is important to determine the reliability of communication within a cone. It is of greater relevance to determine whether the postulated GABA_A receptor/Cl channel (Skrzypek & Werblin, 1983; Murakami, Shimoda, Nakatani, Miyachi, & Watanabe, 1982a,b) is involved in the feedback response and whether other ion channels are modulated by transmitters. It is expected that the basic mechanisms of this synaptic interaction can be related to the functional role of center-surround antagonism in the retina. Furthermore, it will be interesting to compare this cone model to presynaptic inhibition in local (nonspiking) circuits more generally in the nervous system.

CHAPTER 2

MATERIALS AND METHODS

2.1 Retinal Slice Preparation.

Slices were made according to the technique described by Werblin (1978). Larval tiger salamanders, *Ambystoma tigrinum* (Kons Scientific Supply, Germantown, WI), were stored at 5°C under an 8:16 hour light:dark cycle. For light response recordings, before each experiment, an animal was dark adapted for thirty to sixty minutes in an opaque container filled with tap water and covered with a tray and a black cloth. Under dim red illumination, animals were quickly decapitated and pithed, and both eyes were enucleated. One eye was stored in bath solution in darkness at 5°C for later use. The other eye had its cornea and lens removed. The iris was cut away leaving an eyecup. A small (1-2 mm²) section of the eyecup which included the sclera and pigment epithelium was cut and placed sclera side up on a piece of Millipore filter paper (Millipore Corporation, Bedford, MA) secured by Vaseline on a glass slide. After the retina had attached to the filter paper (a few seconds), bath solution was added. The sclera and pigment epithelium were removed and the retina and filter paper were sliced with a razor blade into 150 μm sections. Each section was then rotated 90° and placed on two rows of Vaseline such that all the retinal layers could be viewed under a Zeiss 40X water-immersion objective on a Nikon microscope using an infrared TV camera and monitor. For experiments not requiring dark adaptation, slices were made under normal room illumination and were viewed by light microscopy under a Zeiss 40X water-immersion objective on a Nikon microscope.

2.2 Solutions.

The standard bath solution contained (in mM): 90 NaCl, 2.5 KCl, 3 CaCl₂, 10 HEPES, and 8 Glucose adjusted to pH 7.60 with NaOH (Bader and Bertrand, 1984). In order to better resolve Ca currents, a BaTC bath solution was used containing (in mM): 65 NaCl, 2.5 KCl, 20 BaCl₂, 10 Tetraethylammonium (TEA) bromide, 5 CsCl, 10 HEPES, and 8 Glucose adjusted to pH 7.60 with NaOH. Other changes are described in the text of figure legends. Two pipette solutions were used: a Na-K pipette solution that contained (in mM): 80 KCl, 20 NaCl, 3.5 MgCl₂, 10 HEPES, 1 EGTA, 1.5 Na₃ adenosine 5'-triphosphate (ATP), and 0.1 Na₄ guanosine 5'-triphosphate (GTP) adjusted to pH 7.20 with NaOH (Bader and Bertrand, 1984) and a Cs pipette solution which contained (in mM): 100 CsCl, 3.5 MgCl₂, 5 HEPES, 1 EGTA, and 1.5 ATP adjusted to pH 7.20 with CsOH. ATP, EGTA, and HEPES were obtained from Sigma (Saint Louis, MO). GABA and L-glutamic acid hydrochloride were obtained from Research Biochemicals Incorporated (Natick, MA). The pH of each solution was measured before each experiment with a pH meter (Corning model 240) and adjusted with NaOH and HCl. Solutions were applied at room temperature (21°C to 25°C) by gravity-driven inflow via an eight-way valve and removed by either a reversed aquarium air pump or a peristaltic pump (Pharmacia).

2.3 Whole-Cell Patch-Clamp Recording And Analysis.

Whole-cell pipettes were pulled from glass hematocrit tubes (Western Scientific, Richmond, BC) in two steps on a vertical puller (Kopf model 730, Tujunga, CA). Filled with the CsCl pipette solution, they had tip resistances between 8 and 12 Mohms measured in standard bath solution. The bath reference electrode consisted of a bath solution-filled agar bridge with a chlorided silver wire.

Whole-cell voltage was clamped with an Axopatch 1-C (Axon Instruments, Burlington, CA). Whole-cell currents in the light were filtered at 1 kHz or 500 Hz (-3 dB, four pole low-pass Bessel) and recorded and stored digitally at 1 kHz (12-bit resolution) with a BASIC-FASTLAB system (Indec Systems, Sunnyvale, CA) incorporating an 125 kHz A/D board with opto-isolation and a 286 computer. Fast transient current changes that may require filtering at half the recording rate were not the focus of analysis. Light-elicited currents were filtered at 200 Hz. BASIC-FASTLAB software also generated the voltage-clamp commands and provided programs for analysis of data and drawing of figures. Several successive data points were averaged together where the response changed slowly in time to reduce storage requirements. For illustration, several points at the peak of each capacitance current transient have been removed from some records.

Pipette and bath electrode junction potentials were measured against high-resistance (50 Mohms) 3 M KCl electrodes. Pipette potentials were about 1 mV for the CsCl/NaCl bath combination and about 2 mV for the NaCl/Barium bath combination. Voltage-clamp traces are uncorrected for the potentials.

2.4 Light Stimulation.

All light stimuli were full-field white light steps unless otherwise specified. The maximum intensity (irradiance) was $580 \mu\text{W}/\text{cm}^2$ measured after passage through a light pipe at the level of the slide containing the slices. A lamp (Model 68735, Oriel Corporation, Stratford, CT) connected to a shutter drive control (Model SD-122B, Vincent Associates, Rochester, NY) was the light source. The shutter was controlled by the BASIC-FASTLAB software. Neutral density filters (Oriel Corporation, Stratford, CT) attached to a wheel attenuated the light (between -5.5 attenuation and no attenuation in .5 log unit decrements) before it

reached the slice via a four foot long fiber optic cable. The irradiance values noted in the text and figures represent irradiance measured at the level of the slide.

2.5 Computer Modelling.

To examine electrical communication within a cone photoreceptor, a compartmentalized computer simulation program called *Manuel* (Perkel & Mulloney, 1978; and thanks to David Perkel, UCSF) was used. It consists of a family of programs that reconstruct and simulate simple neural structures. Membrane types, structural compartmentalization, experimental protocol and recording were entered into the program and simulations were carried out. *Manuel* computes cell voltage via integration of total membrane current after calculation of current contributions from voltage-gated currents described in terms of the Hodgkin-Huxley kinetics model (Hodgkin & Huxley, 1952).

Cone properties used for the simulation were obtained from cones filled with 1% Lucifer yellow (Stewart, 1978) via the patch pipette. Filled cells were visualized with a fluorescence epi-illuminator attached to the microscope, photographed at different focal planes, and scrutinized for morphological parameters: total surface area, telodendrite number, telodendrite length and telodendrite diameter. These measurements were converted into surface area by using cylindrical geometry. In brief, each one micron length of the cone was treated as a cylinder with a diameter equal to the width of the cell at that position. Surface area measurements gave approximate values of capacitance which were then entered into the program. Capacitance and input resistance were also measured in many of the cones filled using small voltage commands from -60 mV to -50 mV. Membrane capacitance was determined from current records taken with higher frequency response. Small depolarizing voltage steps were applied to the

membrane, and the current signal was filtered at 1 kHz and sampled digitally at 5 kHz. The area under the transient portion of the current was integrated to determine membrane capacitance. All membranous regions initially had homogeneous properties. Changes in these properties are noted in the text of figure legends.

CHAPTER 3

RESULTS

3.1 Properties of Cones

3.1.1 Morphology of Cones and Simulation of Transmission Within Cones

Tiger salamander cone cell bodies lie close to the OPL and generally do not have an axon leading to a terminal. Instead, the cone synaptic terminal is located in close proximity to the cell body. Most cells types in retinal slices were easily identifiable using light microscopy (Figure 1). The arrow in Figure 1 points to a single cone. Lucifer yellow (molecular weight 457.3; Stewart, 1978) also served as a useful tool to visualize cells. Figure 2 shows photographs at different focal planes of a cone filled with 1% Lucifer yellow via a patch pipette. A composite drawing of the cell is shown in the lower right-hand frame. The cell body, inner segment and outer segment usually filled with Lucifer yellow within seconds of break through while telodendrites filled more slowly. Fluorescing cells were visualized under epi-illumination and rough sketches were drawn (not shown).

3.1.1.1 Morphological and Passive Electrical Parameters

Morphological parameters such as cell diameter, height, telodendrite number and telodendrite diameter were measured from the photomicrographs. Tiger salamander cones had approximately five telodendrites with an average length of $14.5 \pm 11.2 \mu\text{m}$ (mean \pm S.D., $n = 5$) (Figure 3A). Telodendrites had a beaded appearance confirming earlier observations (Lasansky, 1973) and ranged in diameter from .25 to $2 \mu\text{m}$ (best estimate using fluorescence microscopy). In most cases, there was a larger region at the end of the telodendrite. Passive electrical properties were measured from single and double cones and no difference in properties was observed between them. Cone capacitance averaged $39.3 \pm 21.4 \text{ pF}$

Figure 1. Photograph of a tiger salamander retinal slice. All layers of the retina are visible, including the photoreceptor layer (PRL), outer plexiform layer (OPL), inner nuclear layer (INL), inner plexiform layer (IPL), and ganglion cell layer (GCL). The arrow points to a single cone photoreceptor. Modified from Merchant and Barnes, 1992.



Figure 1.

Figure 2. Lucifer yellow fill of a cone photoreceptor. Photographs at different levels of depth of a cone photoreceptor in a retinal slice filled with 1% Lucifer yellow via the patch pipette shown on the left. A composite drawing of the cell and its telodendrites is shown in the lower righthand frame. Modified from Merchant and Barnes, 1991.

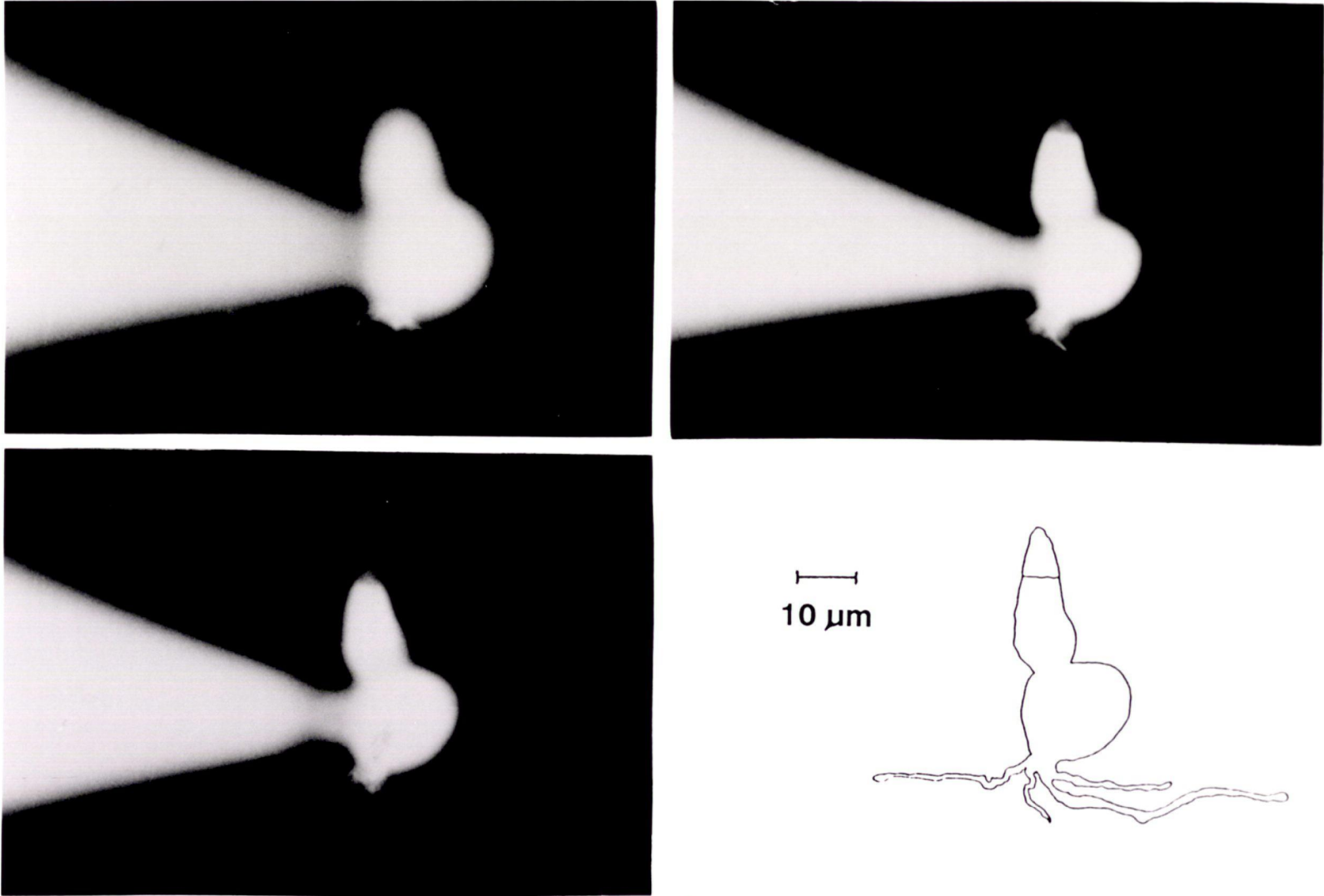
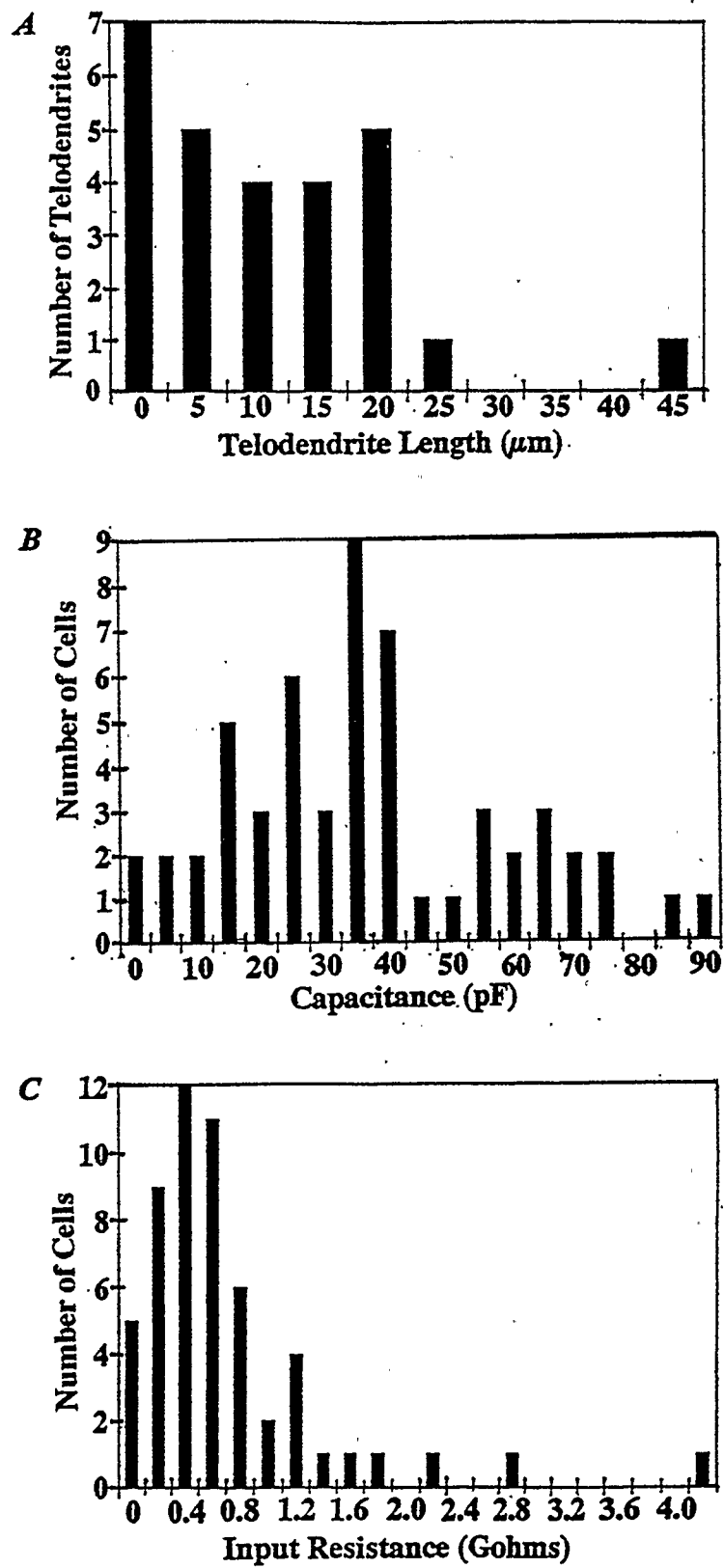


Figure 2.

Figure 3. Morphological and passive electrical properties of cones. *A.* Histogram of telodendrite length measured from composite drawings of Lucifer yellow filled cones (see *Figure 2*; $n = 5$). On average cones had 5 telodendrites with lengths of $14.5 \pm 11.2 \mu\text{m}$ (mean \pm S.D., $n = 5$). Each bin represents the number shown plus $4 \mu\text{m}$. *B.* Histogram of cone cell capacitance ($n = 55$) measured by recording capacitive transients that result from voltage steps from -60 mV to -50 mV . The area under the transient was calculated as the cell capacitance. Average cell capacitance was $39.3 \pm 21.4 \text{ pF}$. The bin width is 5 pF (i.e. $0\text{-}4 \text{ pF}$, $5\text{-}9 \text{ pF}$, $10\text{-}14 \text{ pF}$...). *C.* Histogram of cone cell input resistance ($n = 55$) measured as the steady state current level during the step from -60 mV to -50 mV . Average input resistance was $797.1 \pm 701 \text{ Mohms}$ at -60 mV . The bin width is 0.199 Gohms (i.e. $0\text{-}.199 \text{ Gohms}$, $.2\text{-}.399 \text{ Gohms}$, $.4\text{-}.599 \text{ Gohms}$...). Modified from Merchant and Barnes, 1991.

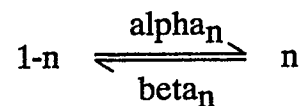
*Figure 3.*

(Figure 3B, $n = 55$) while cone input resistance averaged 797.1 ± 701 Mohms (Figure 3C, $n = 55$).

3.1.1.2 Computer Modelling Of Communication Within A Cone

Simulation of transmission within a cone was carried out using *Manuel*. The cone used in the simulations was simplified. It had a cell body with a capacitance of 20 pF and a single 20 μm long telodendrite of 1 μm diameter ending in a 0.6 pF region. The input resistance at the cell body was about 1.3 Gohms near -40 mV. All membraneous regions initially had homogeneous properties. Changes in these parameters are noted below. Voltage-clamp currents characteristic of cones in slices (Barnes & Hille, 1989; Beech & Barnes, 1989) were measured (see section 3.1.2 on ionic currents). Three of these currents, I_h (a non-selective cation current), I_{Kx} (a standing outward potassium current), and I_{Ca} (calcium current) were fit with Hodgkin-Huxley style gating parameters.

Hodgkin and Huxley (1952) formulated a model to describe channel gating by postulating that gating particles were present in the membrane. If a gating particle in the membrane is represented as n , the voltage- and time-dependent changes of n can be represented by the first order reaction given by



where the particle makes transitions between the permissive (n) and nonpermissive ($1-n$) states with voltage-dependent rate constants alpha_n and beta_n (Hille, 1992, p. 46). If the initial value of the gate opening probability is known, subsequent values can be calculated from a differential equation represented by $dn/dt = \text{alpha}_n(1-n) - \text{beta}_n n$ (Hille, 1992, p. 46). These probabilities can then be used to model the behaviour of a channel. Values for the voltage-dependent time constant (tau_n) and the steady-state probability value (n_∞) can be measured from recordings

of currents. These values are described by $\tau_n = 1 / (\alpha_n + \beta_n)$ and $n_\infty = \alpha_n / (\alpha_n + \beta_n)$. Mean values for α_n and β_n were calculated from recordings (by Barnes & Hille, 1989, and Beech & Barnes, 1989) and fit with the functions in *Manuel*, where $\alpha = [A+BE]/[C+\exp((E+D)/F)]$ and $\beta = [A+BE]/[C+\exp((E+D)/F)]$ in units of msec^{-1} . E was the membrane potential. Values for α , β , the maximum conductance (g_{max}), the Nernst potential (V_{rev}), and the gating exponent (the value that the gate opening probability is raised to) for I_h , I_{Kx} , and I_{Ca} are shown below.

$$I_h: \quad \alpha = \frac{0.05}{1 + \exp[(V+88)/12]} \quad \beta = \frac{0.018}{1 + \exp[(V+18)/(-19)]}$$

$$g_{\text{max}} = 2.2 \text{ nS}, V_{\text{rev}} = -32 \text{ mV}, \text{gating exponent} = 4.$$

$$I_{Kx}: \quad \alpha = \frac{0.07078 + 0.00157(V)}{1 - \exp[(V+45)/(-7)]} \quad \beta = \frac{0.066 - 0.0012(V)}{\exp[(V+55)/5.5] - 1}$$

$$g_{\text{max}} = 1 \text{ nS}, V_{\text{rev}} = -77 \text{ mV}, \text{gating exponent} = 1.$$

$$I_{Ca}: \quad \alpha = \frac{0.26 + 0.0047(V)}{1 + \exp[(V+20)/(-12)]} \quad \beta = \frac{0.02 - 0.0055(V)}{1 + \exp[(V+0)/12]}$$

$$g_{\text{max}} = 1 \text{ nS}, V_{\text{rev}} = 60 \text{ mV}, \text{gating exponent} = 1.$$

These values for the above parameters were entered into the program and simulations of the ionic current I_h , I_{Kx} , and I_{Ca} were carried out.

In the dark, a standing inward current (or dark current) maintains the membrane potential of photoreceptors near -40 mV. Light turns off this inward current and hyperpolarizes photoreceptors to about -60 mV. This light response originating at the cell body was simulated in Figure 4. Continuous measurements of cell body membrane potential (solid trace) and telodendrite membrane potential (dashed trace) were made by *Manuel* and stored. The simulation in Figure 4A

Figure 4. Simulation of a synaptic input at a 1 μm diameter telodendrite during a 30 pA light response. *A.* 30 pA of photocurrent (solid line) is injected at the cell body. A 5 pA input (dashed line) at the telodendrite opposes the cell body input. The solid trace represents measured cell body voltage while the dashed trace represents measured telodendrite voltage. *B.* Simulation as in *A* with 20 pA injected at the telodendrite. *C.* Simulation as in *A* with 40 pA injected at the telodendrite resulting in a calcium spike. *D.* Summary diagram showing coupling ratios from the cell body to the telodendrite and from the telodendrite to the cell body from simulations in *A*, *B*, and *C*. The coupling ratio from the cell body to the telodendrite was 99% and the coupling ratio from the telodendrite to the cell body was 88%. Modified from Merchant and Barnes, 1991.

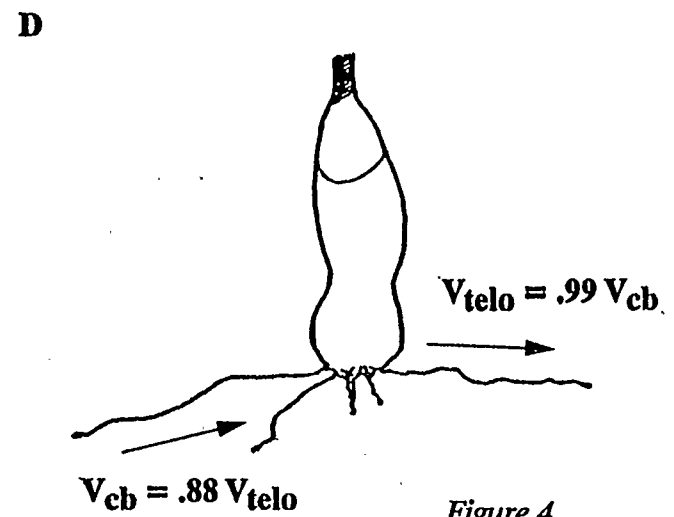
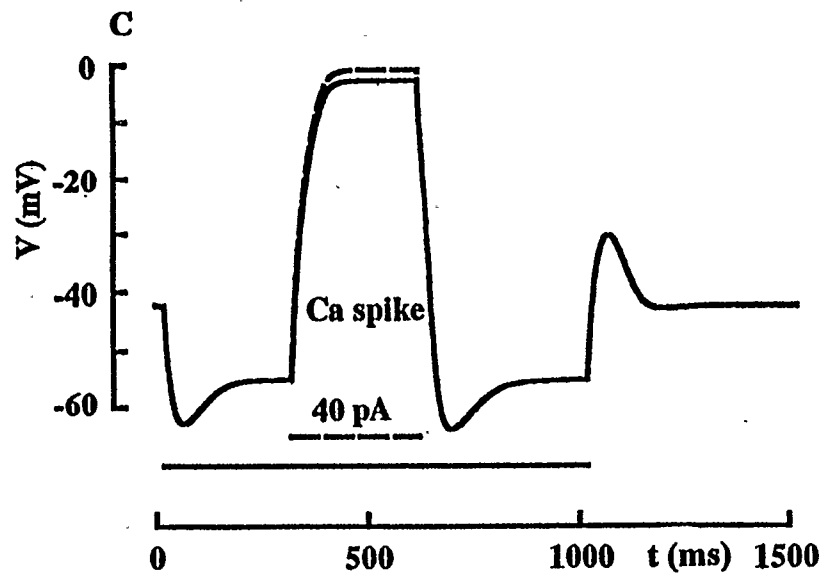
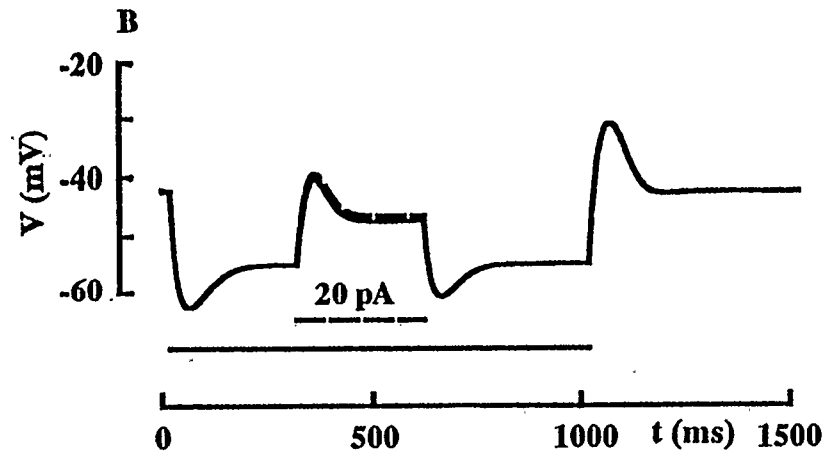
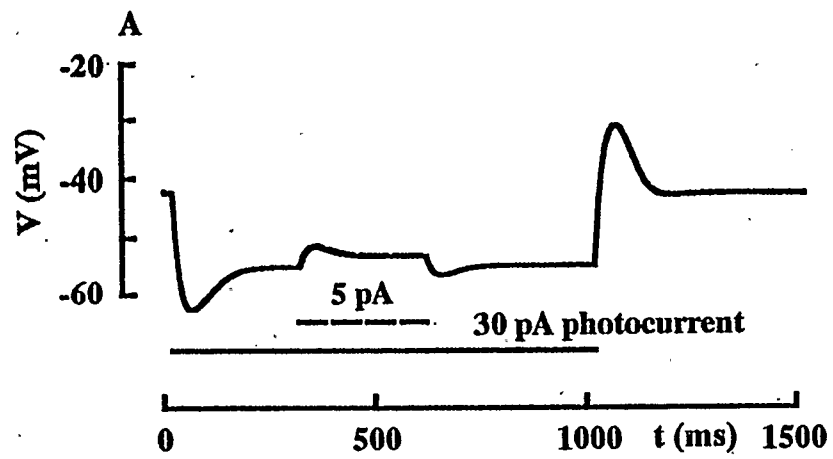


Figure 4.

shows a cell at a resting potential of about -42 mV. A 30 pA current injection lasting for 1 s (indicated in the following figures by the solid line) hyperpolarized the cell body to a potential more negative than -60 mV. The shaping of the response at the beginning and at the end of the photocurrent injection was probably due to the activation of I_h which acts to depolarize the cell. 5 pA of synaptic input (indicated in the following figures by the dashed line) injected at the telodendrite and lasting 300 ms is recorded at the telodendrite and at the cell body (Figure 4A). Using the protocol above, this set of simulations also shows synaptic inputs of 20 pA (Figure 4B) and 40 pA (Figure 4C) injected at the telodendrite. Under these modelled conditions electrical coupling between the cell body and the telodendrite was good in both directions. The coupling ratio for signals originating in the cell body and propagating to the telodendrite is close to 100%. The coupling ratio in the reverse direction is around 88% over the entire voltage range tested, even during the Ca spike initiated in the telodendrite (Figure 4C).

Changes in parameters such as a higher calcium channel density in the telodendrite, a thinner telodendrite, and a strong shunt at the cell body failed to uncouple the cell body and telodendrite. The diameter of the telodendrite (axial resistance) was the main determinant of the degree of coupling between the cell body and telodendrite. Generally, the coupling ratio for signals arising in the cell body and propagating to the telodendrite was around 99% while the coupling ratio in the opposite direction was 88% (Figure 4D). Even though the resistances between the cell body and the telodendrite may be the same, the size of the signal and the properties of the area where the signal is being sent play an important role in determining coupling. These parameters may account for the differences in coupling (see section 4.1.1).

3.1.1.3 Conclusion

Reasonable morphological and electrical parameters that would lead to significant uncoupling of the cone telodendrite and cell body were not found. Therefore, a signal arising distally in the telodendrite would be reliably transmitted to the cell body. Communication was found to be good bidirectionally. Thus if the negative feedback signal from horizontal cells was transmitted through the telodendrites, the cell body would receive almost 100% of the signal which might then be transmitted to its second order neurons to change their receptive fields.

3.1.2 Ionic Currents In The Inner Segments Of Cones

Several ionic currents characteristic of cones (Barnes & Hille, 1989) were recorded under bright illumination using the whole-cell patch-clamp technique. These included calcium and calcium-activated currents (I_{Ca} , $I_{Cl}(Ca)$, and $I_{K}(Ca)$), potassium currents (I_K and I_{Kx}) and a non-selective cation current (I_h). Each will be discussed below.

3.1.2.1 I_{Ca} , I_{Ca} -Activated Currents, And pH

Cone photoreceptors have L-type (Nowycky, Fox, & Tsien, 1985) calcium channels that are activated at potentials near -40 mV and do not show inactivation. These currents are better resolved when the external solution contains 5 mM Ba^{2+} and 0 mM Ca^{2+} . Figure 5A shows inward barium current activated by depolarizing voltage steps. The current was non-inactivating during the voltage step. Only steps to +10 mV are shown. The current-voltage (I-V) relation shows currents elicited at potentials up to +90 mV (Figure 5B). Current activated at -40 mV and reached a peak of 75 pA at -30 mV ($n = 2$).

Isolated rod and cone calcium channels have been shown to be sensitive to extracellular pH changes (Barnes & Bui, 1990; Mahmud & Barnes, 1992). Cones in retinal slices had a similar pH dependence exhibiting a 12 mV shift in activation

Figure 5. Barium currents of cones. *A.* Series of barium currents from a cone in 5 mM Ba²⁺ at pH 7.60 in response to 8 depolarizing steps in 10 mV increments. The data were filtered at 500 Hz and sampled at 1 kHz. Only currents to steps up to 10 mV are shown for clarity. From Merchant and Barnes, 1991. *B.* Barium I-V relation of cone in *A.* Standard bath solution with 5 mM BaCl₂ and 0 mM CaCl₂, pH 7.60. Na-K pipette solution, pH 7.20.

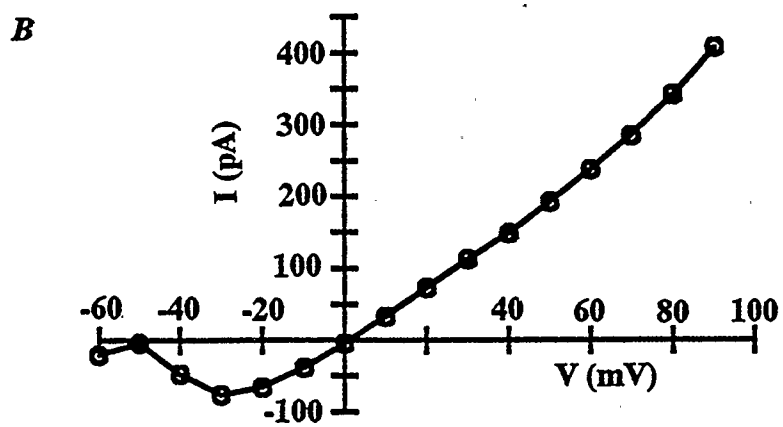
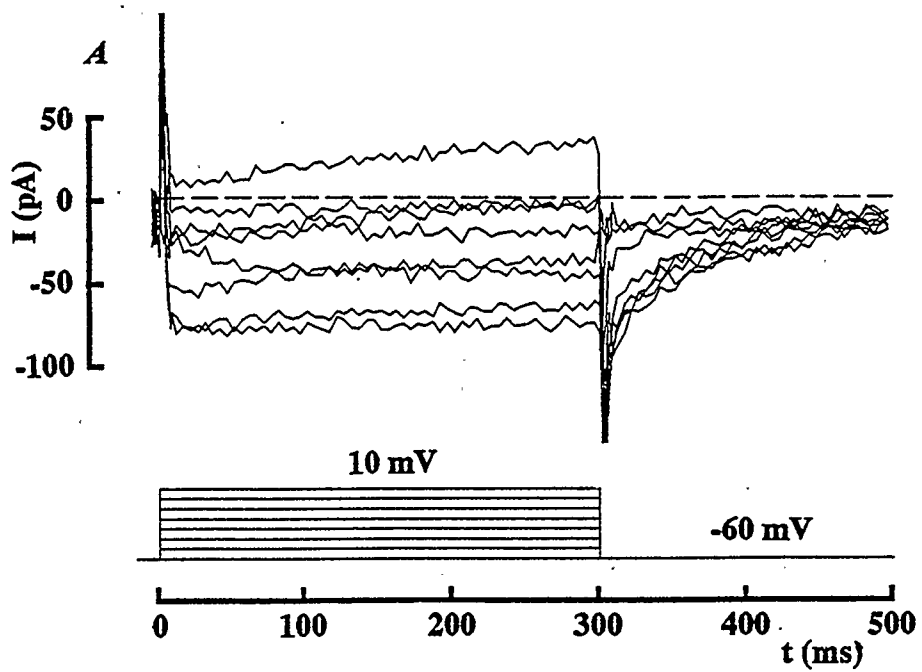


Figure 5.

with changes of pH_O . I-V relations of barium (20 mM) current at pH_O 7.0 and pH_O 7.8 in Figure 6A reveal that current activated at a more negative potential in alkaline pH_O and at a more positive potential in acidic pH_O relative to control pH of 7.60. The activation curves in Figure 6B were derived from the I-V relations in Figure 6A and show a shift of the midpoint along the voltage axis.

Two calcium-activated currents were also recorded: a calcium-activated chloride current ($I_{Cl}(Ca)$) and a calcium-activated potassium current ($I_K(Ca)$) (Figure 7). Their calcium dependency was demonstrated in a previous study in which activation of these currents was large in the potential range where I_{Ca} was large, activation was less when the pipette solution contained calcium chelators, and no activation when Ca channels were blocked (Barnes & Hille, 1989). Voltage steps to potentials between -60 mV and -20 mV evoke large slowly activating inward currents that also produce very large, long lasting tail currents (Figure 7A). Barnes and Hille (1989) showed that the tail currents had a reversal potential near 0 mV when internal chloride concentration was 104 mM Cl^- and a reversal potential of -43 mV when internal chloride concentration was 14 mM Cl^- (i.e. 90 mM gluconate $^-$). If the channel was impermeable to cations and gluconate the predicted reversal potential should have shifted from 1.4 mV to -49.8 mV. The smaller shift in the observed reversal potential was accounted for if Cl^- were 14 times more permeable than Na^+ and K^+ or if Cl^- were 17 times more permeable than gluconate (Barnes & Hille, 1989). This suggests that the tail currents observed in Figure 7A are probably $I_{Cl}(Ca)$.

$I_{Cl}(Ca)$ tail currents were observed in 95 out of 109 cones tested for the current. Peak tail current for ten such cells was 661.9 ± 232.1 pA (preceding step command was -20 mV, mean \pm SD). The inward currents during the voltage step represent a mixture of I_{Ca} and $I_{Cl}(Ca)$. The long lasting (>4 s) tail currents

Figure 6. Modulation of barium current by changes of extracellular pH. *A.* The whole-cell barium I-V relation at pH 7.0 shifts negative along the voltage axis when pH is changed to 7.8. Standard bath solution with 5 mM BaCl₂ and 0 mM CaCl₂, pH 7.60. Na-K pipette solution, pH 7.20. *B.* Boltzmann fit activation curves derived from the I-V relations in *A.* For pH 7.0, the midpoint of activation was -15 mV and the slope factor was 5.7. For pH 7.8, the midpoint of activation was -25.4 mV and the slope factor was 5.2. The midpoint of activation shifts negative by approximately 10 mV in the range of pH 7.0 to 7.8. Modified from Merchant and Barnes, 1992.

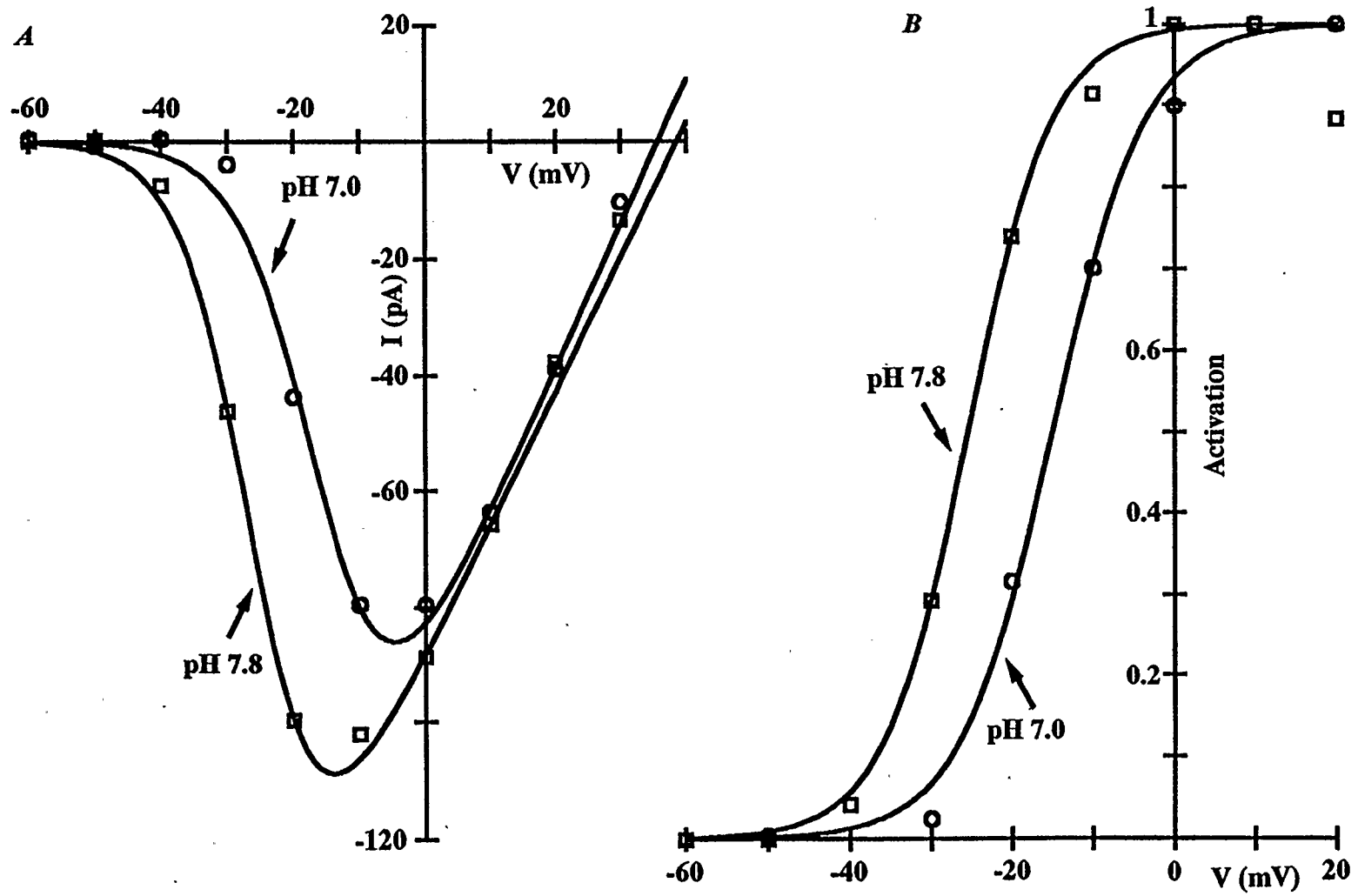


Figure 6.

Figure 7. Whole-cell currents showing I_K , $I_{K(Ca)}$, and $I_{Cl(Ca)}$. *A.* Calcium-activated potassium current ($I_{K(Ca)}$) was activated by depolarizing a single cone from a holding potential of -60 mV to potentials ranging from -40 mV to 60 mV in 10 mV steps for 200 ms. Calcium-activated chloride current ($I_{Cl(Ca)}$) was activated by depolarizing the cone to potentials ranging from -40 mV to 60 mV in 10 mV steps for 200 ms. Tails show a small amount of current at -50 mV that is saturated at -20 mV and is virtually non-existent at 70 mV. I_K is observed at potentials above 70 mV. Standard bath solution, pH 7.60; Na-K pipette solution, pH 7.20. *B.* $I_{K(Ca)}$ and $I_{Cl(Ca)}$ had N-shaped steady-state I-V relations. Whole-cell current is described by the circles and $I_{Cl(Ca)}$ tail currents 50 ms after the end of the voltage step are shown as squares.

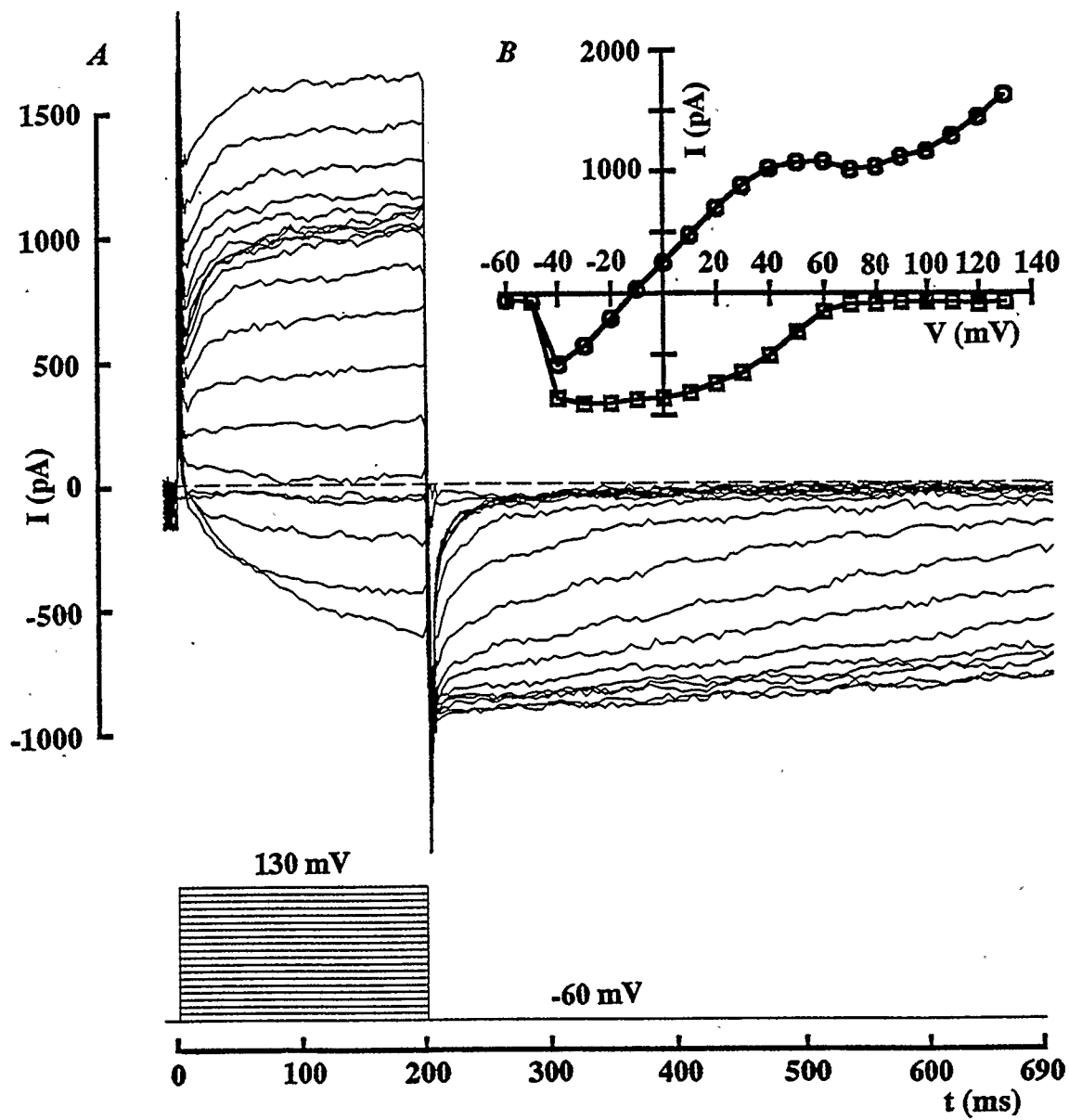


Figure 7.

represent $I_{Cl}(Ca)$ and decay as residual calcium concentration returns to normal levels. As such, tail current serve as assays for changes in calcium concentration.

Large outward currents developed with depolarizations above 0 mV (Figure 7A). These currents increased in amplitude, reached a plateau, and then increased in amplitude again. Currents before the plateau represent $I_{K}(Ca)$, outward $I_{Cl}(Ca)$, and I_K while currents above the plateau represent I_K . Both $I_{Cl}(Ca)$ and $I_{K}(Ca)$ have N-shaped I-V relations (circles) (Figure 7B) suggesting calcium dependence. Steady-state $I_{K}(Ca)$ in ten cells was 1103.1 ± 594.2 pA at +50 mV and was recorded in 68 out of 93 cells tested. The squares in Figure 7B represent tail current 50 ms after the voltage step and also exhibit a calcium dependence (see range of calcium current activation in Figure 6A) The circles represent the steady-state current during the voltage step.

3.1.2.2 I_K

A delayed rectifier type of potassium current is present in cones. It is activated by depolarization and does not inactivate during a short voltage step. This current was observed at high voltages when the calcium-activated currents have deactivated. Figures 7A and 7B show potassium current at potentials larger than +70 mV. In 126 out of 127 cells studied, some outward potassium current was always observed. It had a steady-state amplitude of 1370 ± 688.6 pA at a potential of +80 mV. This current probably serves to prevent large depolarizations of the photoreceptor.

3.1.2.3 I_h and I_{Kx}

Two currents important in controlling the photoreceptor voltage include I_h and I_{Kx} (Beech & Barnes, 1989). I_h is a non-selective cation current activated by hyperpolarization. This current was pharmacologically isolated by Barnes and Hille (1989) by blocking K channels (using 30 mM TEA), Ca channels (using 6 mM

Co^{2+}), and Ca-activated channels. The reversal potential of the current was near -32 mV suggesting a small preference for K^+ over Na^+ (Barnes & Hille, 1989). I_h is represented in Figure 8A by the traces that are below the dashed line. I_h had a steady-state amplitude at -95 mV of 232.1 ± 65.8 pA in ten cells and was observed in 52 out of 61 cells tested. Although not evident in the steady-state I-V relation in Figure 8B, I_h is probably inwardly rectifying and probably opposes photoreceptor hyperpolarization.

I_{Kx} was more difficult to resolve without pharmacological isolation. Beech and Barnes (1989) isolated I_{Kx} by blocking I_h (using 5 mM Cs^+) and I_{Ca} (using 0.1 mM Cd^{2+}) and showed that it reversed between -70 mV and -80 mV. I_{Kx} is a standing outward potassium current that is shut off by hyperpolarization and slightly resolveable in the traces above the dashed line in Figure 8A. It was resolveable in 15 of 61 cells tested although it was probably present in most of the cells tested.

3.1.2.4 Conclusion

The ionic currents of cones recorded in retinal slices correspond well with previously published recordings of isolated cones with the exception that $I_{Cl(Ca)}$ was larger in amplitude in retinal slices. Changes of pH modulate Ca channels of cones by shifting their activation curves along the voltage axis.

Figure 8. I_h and I_{Kx} in a voltage-clamped cone. *A.* I_h is activated by hyperpolarizing a single cone to potentials ranging from -75 mV to -145 mV in 10 mV steps for 300 ms from a holding potential of -40 mV. Traces below the dashed line at 0 pA represent I_h . I_{Kx} is deactivated by hyperpolarizing the same cone from the holding potential to potentials ranging from -45 mV to -65 mV in 10 mV steps for 300 ms. Traces above dashed line at 0 pA represent I_{Kx} decaying with hyperpolarization. Standard bath solution, pH 7.60. Na-K pipette solution, pH 7.20. From Merchant and Barnes, 1991. *B.* I-V relation showing standing Kx current between -30 and -60 mV and inward h current at more negative potentials.

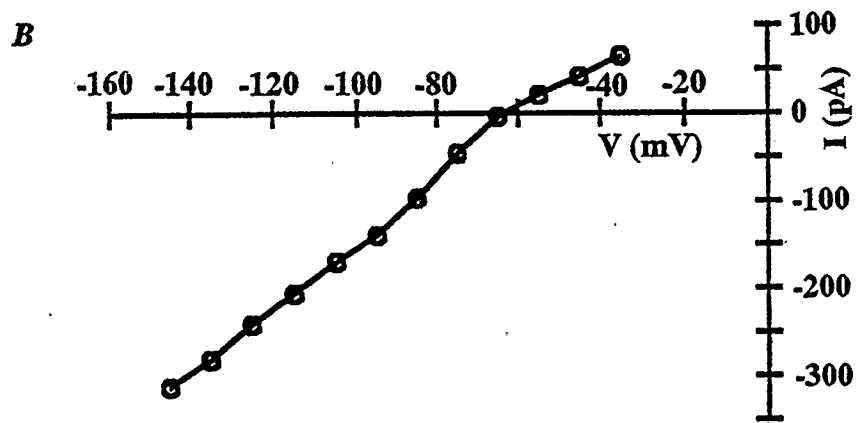
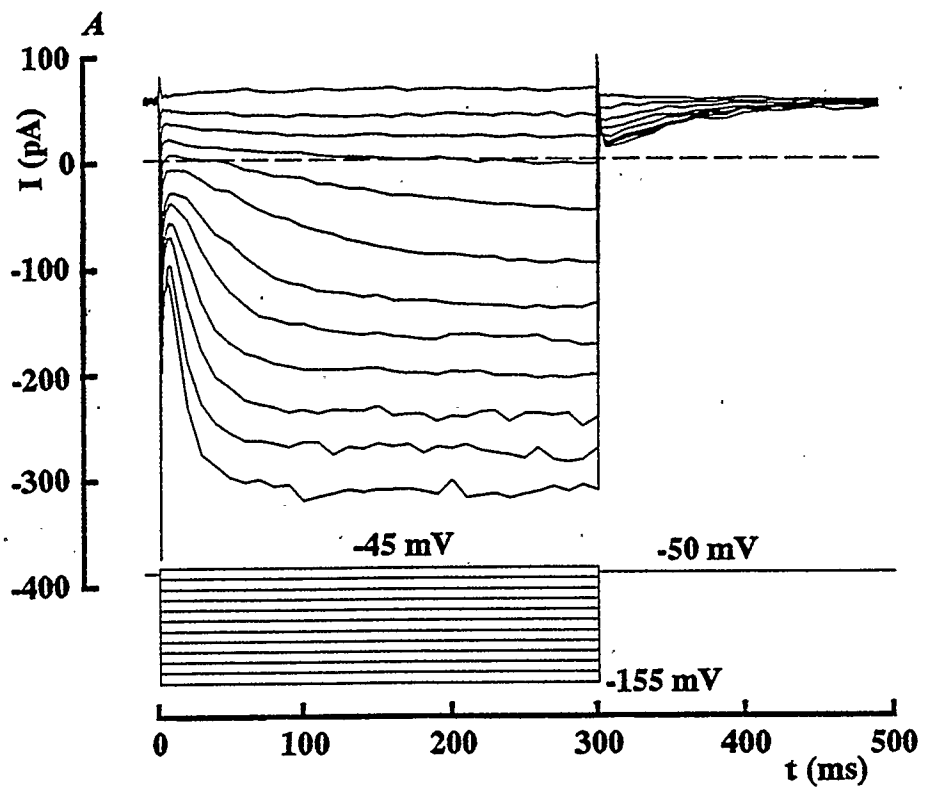


Figure 8.

3.1.3 The Cone Light Response

The cone light response is made up of two components that are dissected out under different levels of background light. Under dark adapted conditions, a step of light evokes the response shown in Figure 9. A 500 ms step of broad field illumination ($580 \mu\text{W}/\text{cm}^2$) results in a reduction of standing inward current 100 ms after the light step. This reduction is maintained 250 ms after the termination of light, after which there is a sharp increase in the amount of inward current. The peak response measured at the brightest intensity averaged 23.7 ± 17.4 pA in amplitude ($n = 4$). The current undershoot at the termination of the light response may be due to feedback from horizontal cells (see section 3.3.2).

3.1.3.1 Log Light Intensity Versus Current

The photoreceptor light response increases in amplitude with increasing intensity of light. Figure 10A shows cone photocurrents at different intensities of light that were 500 ms in duration. Reduction of standing inward current was observed at intensities above -3.0 log units. Complete suppression of the standing inward current was observed with the brightest light stimulus ($580 \mu\text{W}/\text{cm}^2$). The intensity versus photocurrent relation (circles) shown in Figure 10B is fit with the Naka-Rushton function described by $I/I_{max} = 1/(1+[11.22/Intensity]^{1.1})$. The responses show saturation at intensities above $100 \mu\text{W}/\text{cm}^2$. Half-maximal response intensity was $11.22 \mu\text{W}/\text{cm}^2$.

3.1.3.2 Wavelength Dependence

Cone photoreceptors in salamander retina have been shown to be maximally responsive to wavelengths of light near 620 nm (Attwell, Wilson, & Wu, 1984). Maximal response at the peak of the light response was found to be near 600 nm with responses becoming smaller at either side of this wavelength (Figure 11A). The spectral response curve is shown in Figure 11B (circles) as is a nomogram

Figure 9. Photocurrent of one member of a dark-adapted double cone. The cell was held at -60 mV to match the holding potential of cells from which whole-cell currents were recorded in the light. A bright ($580 \mu\text{W}/\text{cm}^2$) broad field light step lasting 500 ms elicited a 20 pA current response. Average of 10 responses. Standard bath solution, pH 7.60; CsCl pipette solution, pH 7.20.

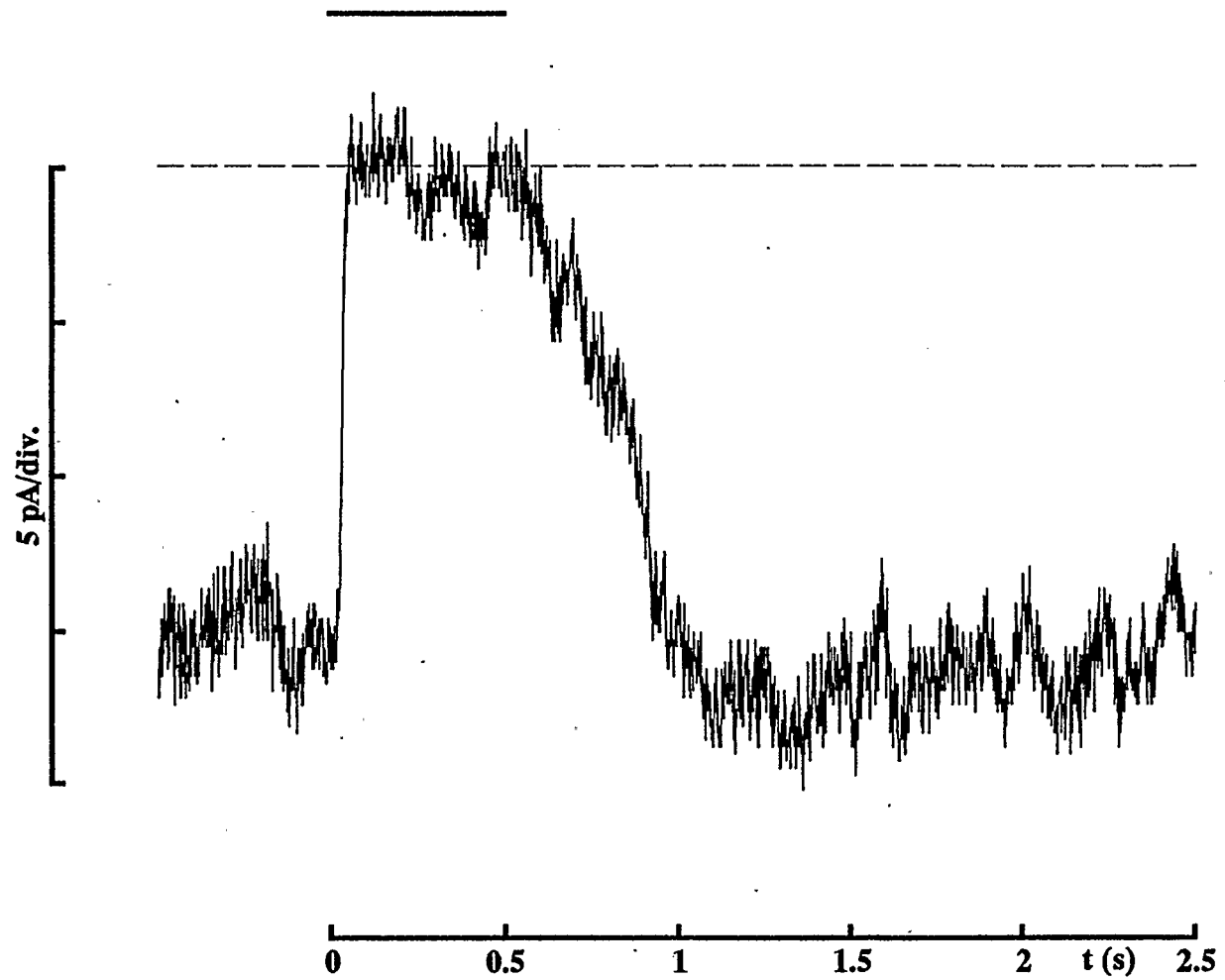


Figure 9.

Figure 10. Photocurrents of a dark-adapted single cone at varying intensities of light. *A.* Responses of a single cone at a holding potential of -60 mV to broad field illumination ranging from 0.0 log unit attenuation ($580 \mu\text{W}/\text{cm}^2$) to -4.0 log unit attenuation ($0.0058 \mu\text{W}/\text{cm}^2$). Duration of light step was 500 ms for each intensity. Standard bath solution, pH 7.60; CsCl pipette solution, pH 7.20. *B.* Relation describing relative response and light intensity (circles). The data were fit with the Naka-Rushton function (solid line) described by $I/I_{max} = 1/(1 + [11.22/Intensity]^{1.1})$.

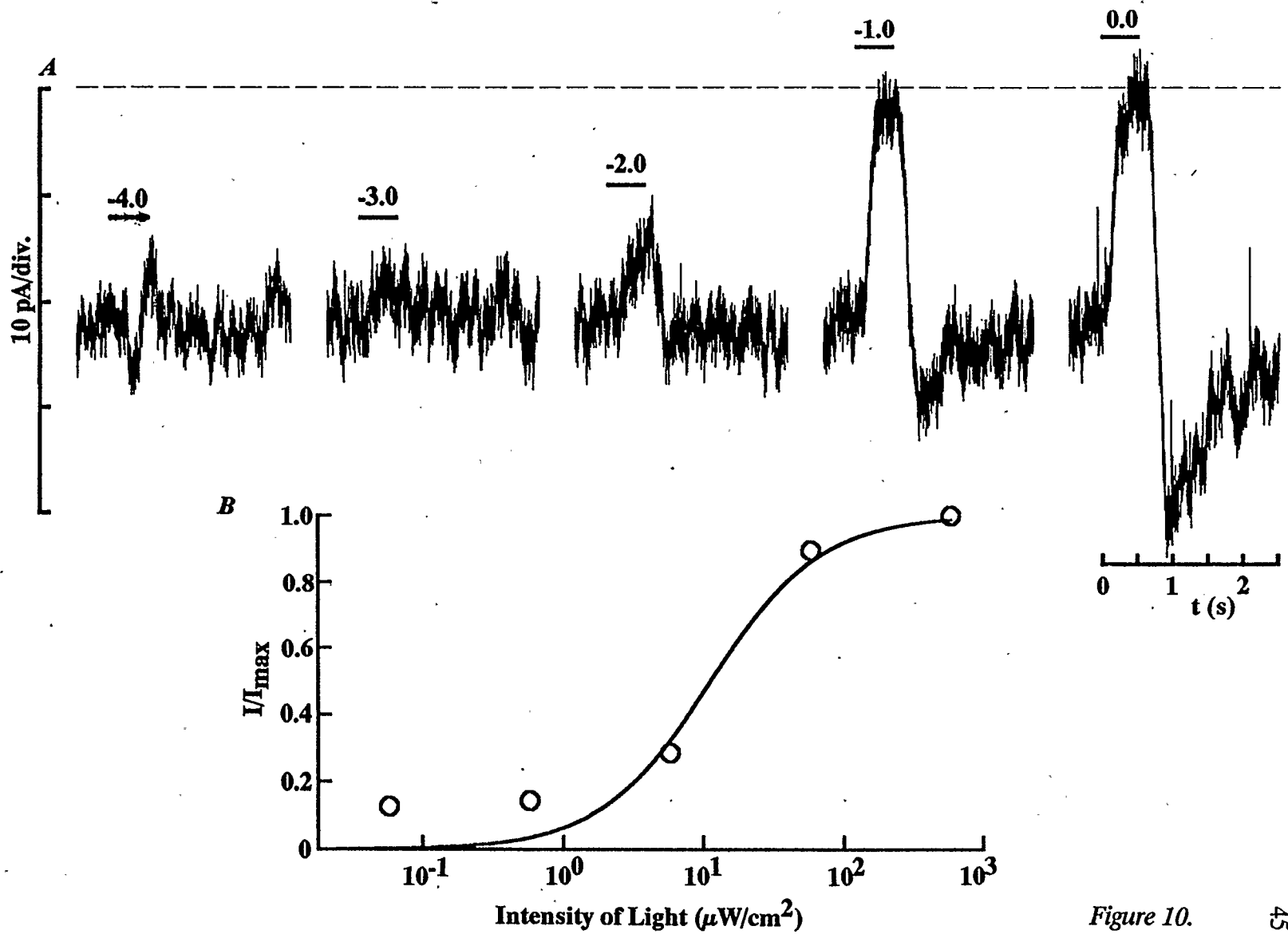


Figure 10.

Figure 11. Cone light responses as a function of wavelength of light. *A.* Responses to various wavelengths (range 400.0 to 700.0 nm) of light were elicited from one member of a dark-adapted double cone held at -60 mV. Duration of light step was 500 ms. The peak response occurred at 600 nm. Each response is an average of 2 responses. Wavelength/bandwidth of each filter were: 400.0 nm/10 nm; 450.8 nm/0.9 nm; 499.5 nm/9 nm; 550.5 nm/9 nm; 600.0 nm/10 nm; 649.5 nm/8 nm; 700.5 nm/11 nm. Standard bath solution, pH 7.60; Na-K pipette solution, pH 7.20. *B.* Peak currents during the light step were normalized and plotted as percentage of the maximum response at 600 nm. The spectral sensitivity data for the cone were compared to a nomogram with a λ_{max} of 600 nm taken from Dartnall (1958). The nomogram was constructed with the absorption spectrum of frog visual pigment 502 (visual purple) at 20°C.

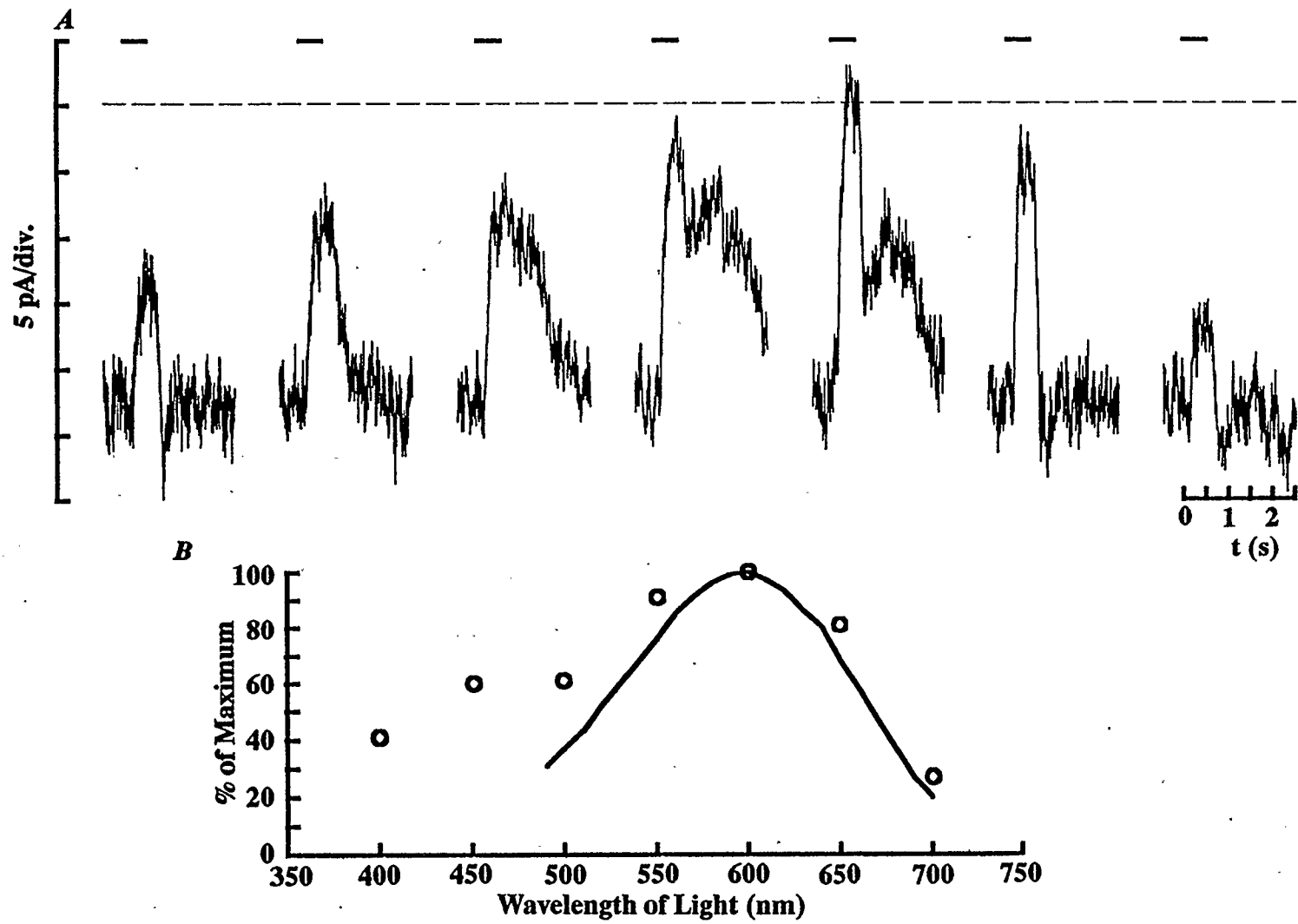


Figure 11.

constructed with the absorption spectrum of frog visual pigment 502 (visual purple) at 20°C (Dartnall, 1958). The responses below 500 nm don't fit well on the nomogram. This is probably because the cone responded not only to the wavelength of light but to its brightness as well. Responses at shorter wavelengths were larger than expected from the nomogram. This may be due to the adaptive state of the cone. Under dark-adapted conditions, the cone may respond strictly to the brightness of the light, irrespective of wavelength. A partially light-adapted cone may respond to brightness and wavelength, thus showing a peak response at 600 nm and small, but significant, responses at shorter wavelengths. It is important to note that the nomogram is of visual pigment 502 (or rhodopsin). The spectral response function in Figure 11 was of a cone which has different visual pigments (Dowling, 1987, p. 195).

3.1.3.3 Conclusion

Cones in retinal slices voltage clamped with patch electrodes are maximally responsive to bright light stimuli in the range from 600 to 650 nm.

3.2 Feedforward transmission

3.2.1 Light-Elicited Currents Of Second-Order Cells

Second-order cells of photoreceptors include horizontal cells, hyperpolarizing (OFF) bipolar cells, and depolarizing (ON) bipolar cells. Their responses are combinations of inputs from rods and cones.

3.2.1.1 Horizontal Cells And OFF-Bipolar Cells

Horizontal cells and OFF-bipolar cells hyperpolarize to light and under voltage clamp show a reduction in standing inward current. Figure 12A represents currents elicited upon depolarization of a horizontal cell from a holding potential of -60 mV. The I-V relation is shown in Figure 12B. Currents from L-type Ca channels were measured in isolated cat horizontal cells (Ueda, Kaneko, & Kaneda, 1992) as were currents from L- and T-type Ca channels measured in cultured white bass horizontal cells (Sullivan & Lasater, 1992). These types of Ca currents were not resolvable under the recording conditions here. Figure 12C demonstrates how the horizontal cell light response is a combination of rod and cone inputs. The upper trace is a cone light response which lasts only as long as the light is on. A rod response in the middle trace, even to a shorter step of light, lasts for up to 10 seconds. Fain and Dowling (1973) found that bright light-induced hyperpolarizations of mudpuppy rods maintained seconds after the light stimulus was turned off. They suggest that this may be due to increased sensitivity of rods as compared to cones. Both rod and cone responses in Figure 12C were combined in the horizontal cell response with the cone and rod components during the light-step and the rod response only after the light step (lower trace). The sharp peak inward current is the generation of the feedback signal by the horizontal cell and will be discussed in section 3.3.2.

Figure 12. Whole-cell and light-elicited properties of a horizontal cell. *A.* Whole-cell currents were elicited by depolarizing the cell from a holding potential of -60 mV in 10 mV increments. Standard bath solution, pH 7.60; Na-K pipette solution, pH 7.20. *B.* Steady-state I-V relation of the currents in *A.* *C.* The horizontal cell response (below) is a combination of cone (top; average of 10 responses) and rod (middle; not averaged) inputs. Duration of the light step for the cone and horizontal cell was 500 ms. Duration of the light step for the rod was 50 ms. Cone, standard bath solution, pH 7.60; CsCl pipette solution, pH 7.20. Rod and horizontal cell, standard bath solution, pH 7.60; Na-K pipette solution, pH 7.20. Light intensity in $58 \mu\text{W}/\text{cm}^2$ for all. *C* modified from Merchant and Barnes, 1992.

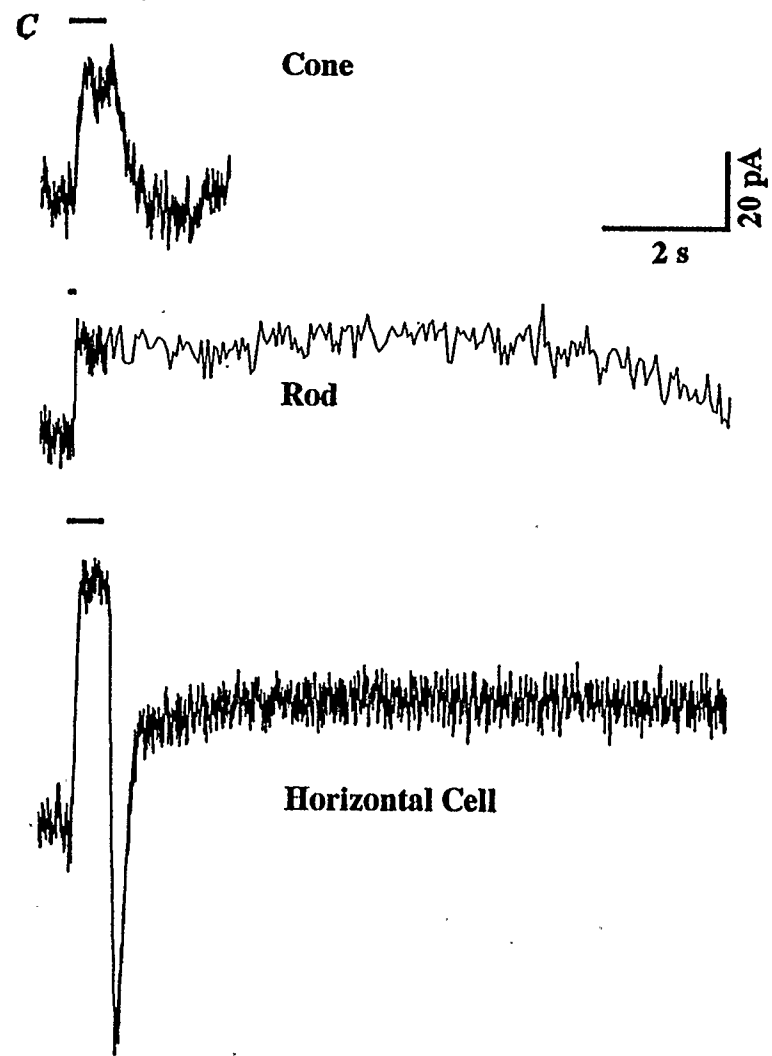
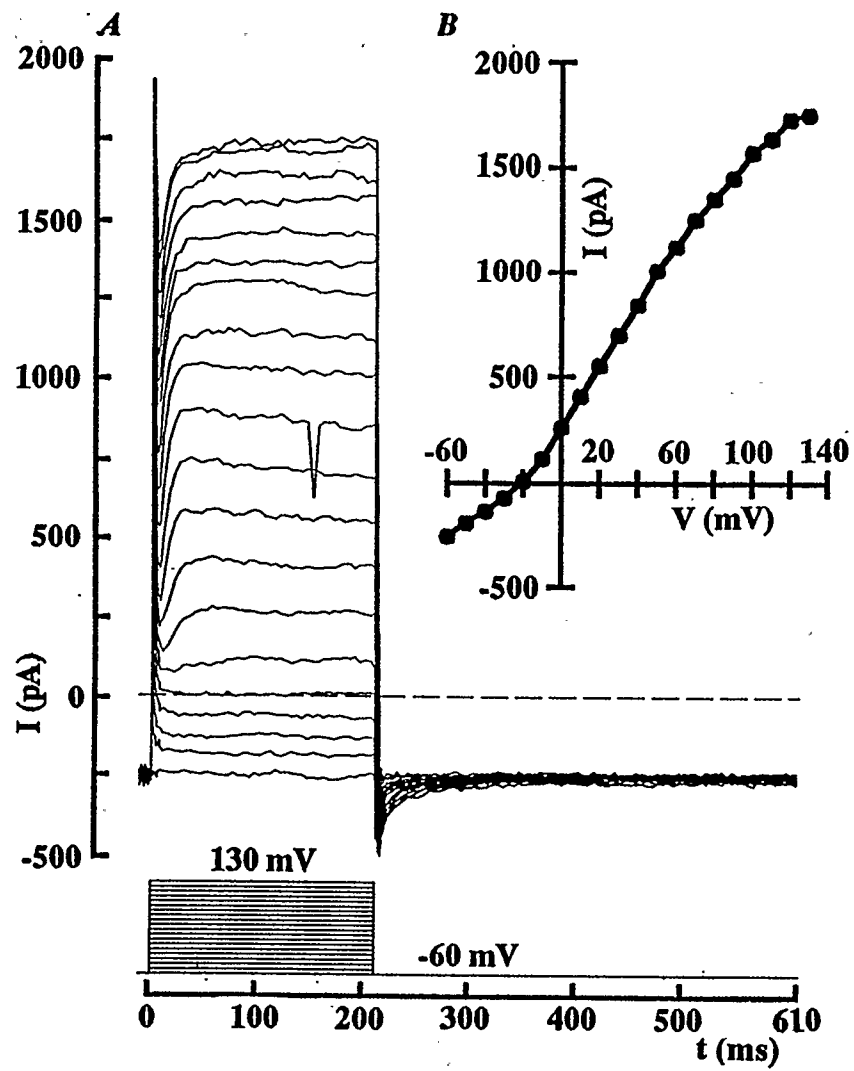


Figure 12.

The amplitude of horizontal cell responses depends upon the intensity of the light step. Figure 13A shows horizontal cell response at varying intensities of light. Notice that the rod component persisted well after brighter steps of light. Figure 13B shows normalized current during the light step (circles) and current after the light step (squares) normalized to the peak current during the light step. The lines joining the symbols are Naka-Rushton fits described by $I_{(cone)}/I_{max(cone)} = 1 / (1 + [0.064/Intensity]^{.58})$ and $I_{(rod)}/I_{max(cone)} = .467 / (1 + [0.19/Intensity]^{2.41})$. Half-maximal response intensities in the cone and in the rod were 0.064 and $0.19 \mu\text{W}/\text{cm}^2$, respectively.

3.2.1.2 ON-Bipolar Cells

The I-V relation of an ON-bipolar cell is shown in Figure 14A. Currents were elicited by depolarizing the cell from a holding potential of -60 mV. Most of the current was outwardly rectifying as demonstrated in the I-V relation in Figure 14B. A 500 ms light step ($58 \mu\text{W}/\text{cm}^2$) resulted in the development of 60 pA of inward current in this ON-bipolar cell. Some residual inward current was observed for about one second after the light step probably due to the input from rods (see section 3.2.1.1 on rod input to horizontal cells).

As in horizontal cells and OFF-bipolar cells, the responses of ON-bipolar cells increase with increasing intensities of light. Figure 15A shows a series of bipolar cell responses at different intensities of light. The amount of light-elicited inward current increased and reached saturation at the brightest intensities. This is further reflected in the intensity versus response curve in Figure 15B where normalized peak current at different intensities was fit with a Naka-Rushton function described by $I/I_{max} = 1 / (1 + [0.83/Intensity]^{.94})$. The half-maximal response intensity was $0.83 \mu\text{W}/\text{cm}^2$.

Figure 13. Light-elicited horizontal cell currents at varying intensities of light. *A.* Photocurrents were generated with broad field illumination of varying intensities (0.058 to 58 $\mu\text{W}/\text{cm}^2$). Responses at -4.0 and -3.0 log unit intensity are averages of 4 responses; responses at -2.0 and -1.0 log unit intensity are not averaged. Duration of the light step at each intensity was 500 ms. Standard bath solution, pH 7.60; Na-K pipette solution, pH 7.20. *B.* Normalized peak current during (circles) the light step and after (squares) the light step were plotted against light intensity. The peak current after the light step was normalized to the peak current during the light step. The data were fit with Naka-Rushton functions described by $I(\text{cone})/I_{\text{max}}(\text{cone}) = 1 / (1 + [0.064/\text{Intensity}]^{.58})$ and $I(\text{rod})/I_{\text{max}}(\text{cone}) = .467 / (1 + [0.19/\text{Intensity}]^{2.41})$.

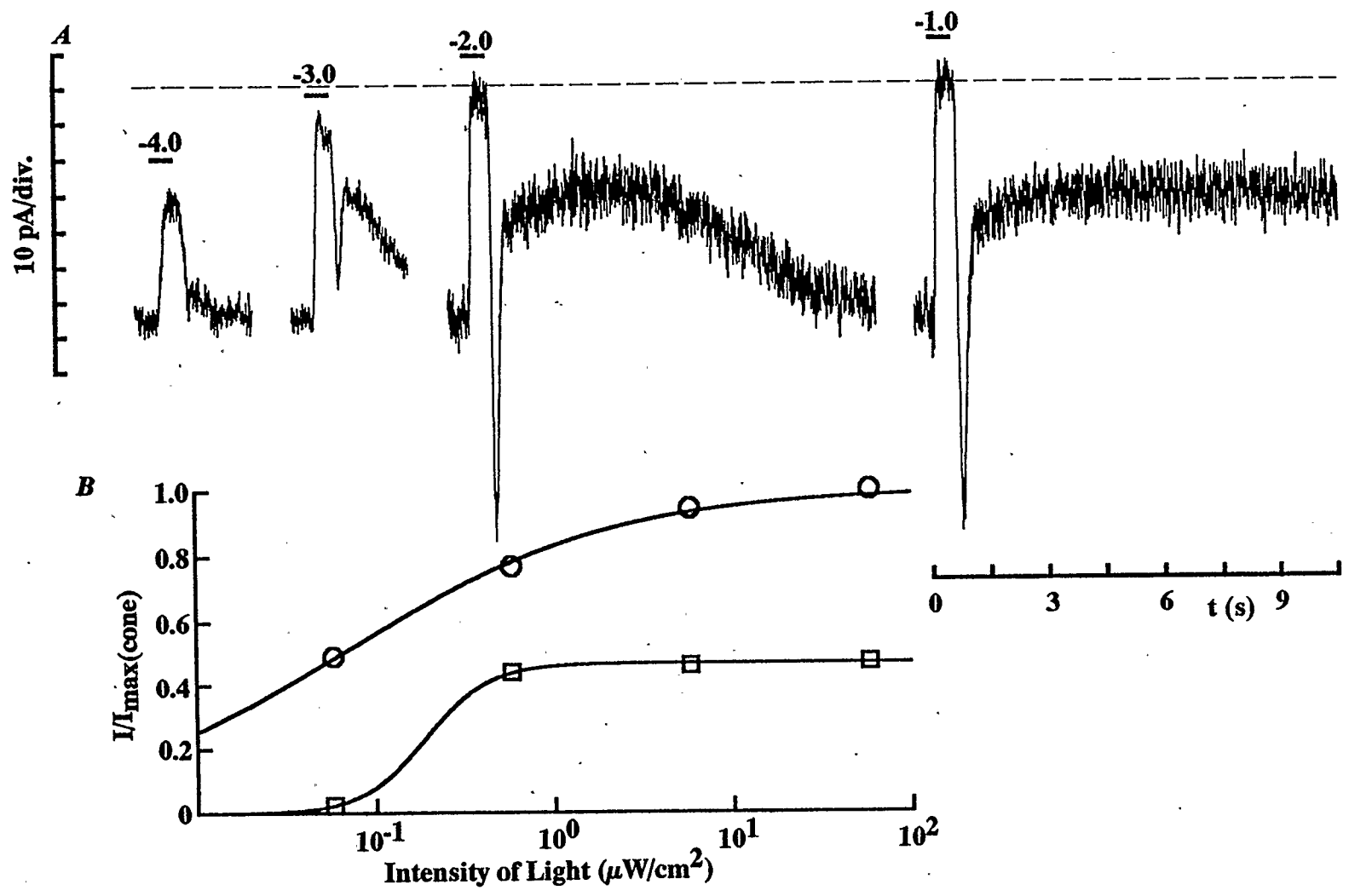


Figure 13.

Figure 14. Whole-cell and light-elicited properties of an ON-bipolar cell. *A.* Whole-cell currents were elicited by depolarizing the cell from a holding potential of -60 mV in 10 mV increments. Standard bath solution, pH 7.60; Na-K pipette solution, pH 7.20. *B.* Steady-state I-V relation of the currents in *A.* *C.* A 500 ms light step ($58 \mu\text{W}/\text{cm}^2$) elicited an inward response that had components of cone and rod inputs.

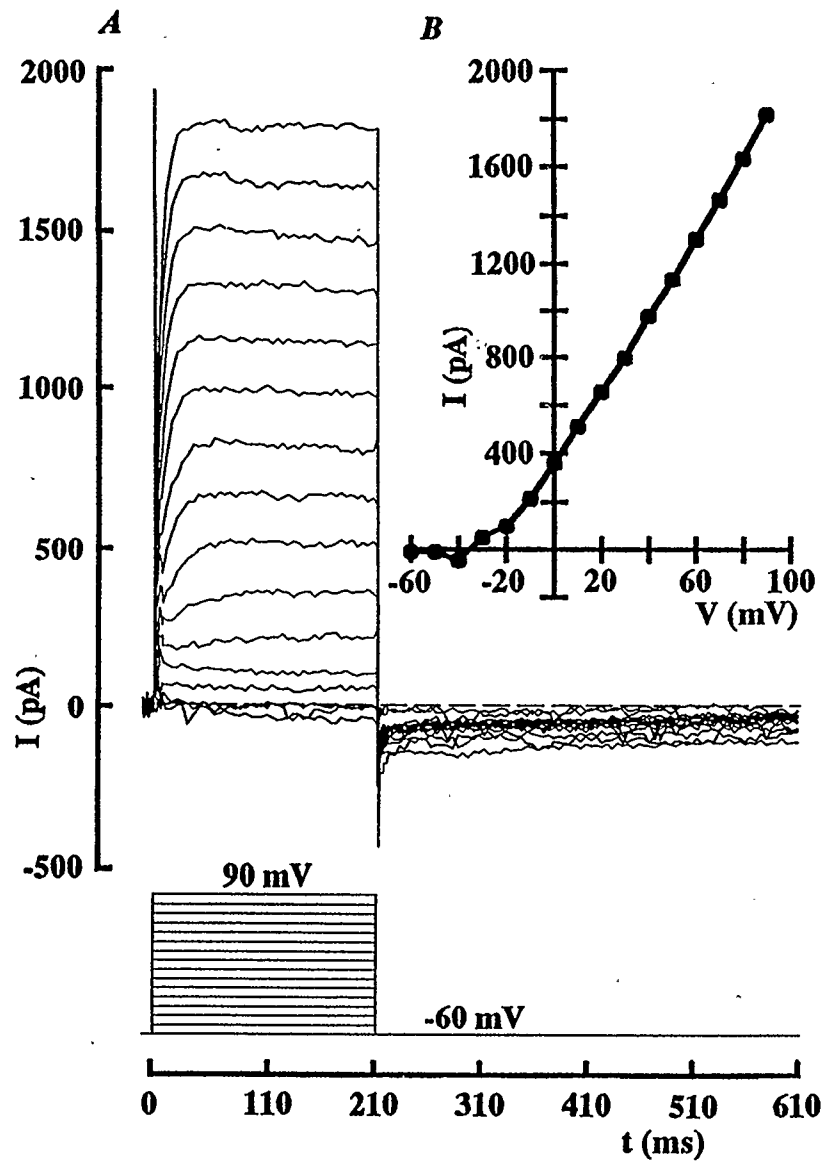


Figure 14.

Figure 15. Light-elicited ON-bipolar cell currents at varying intensities of light. *A.* Light-elicited currents of the cell held at -60 mV were generated with broad field illumination of varying intensities (0.058 to 580 $\mu\text{W}/\text{cm}^2$). Each response is an average of 5 responses. Duration of light step at each intensity was 500 ms. Standard bath solution, pH 7.60; Na-K pipette solution, pH 7.20. *B.* Peak current during the light step were plotted against intensity of light. The data were fit with a Naka-Rushton function described by $I/I_{max} = 1 / (1 + [0.83/Intensity]^{94})$.

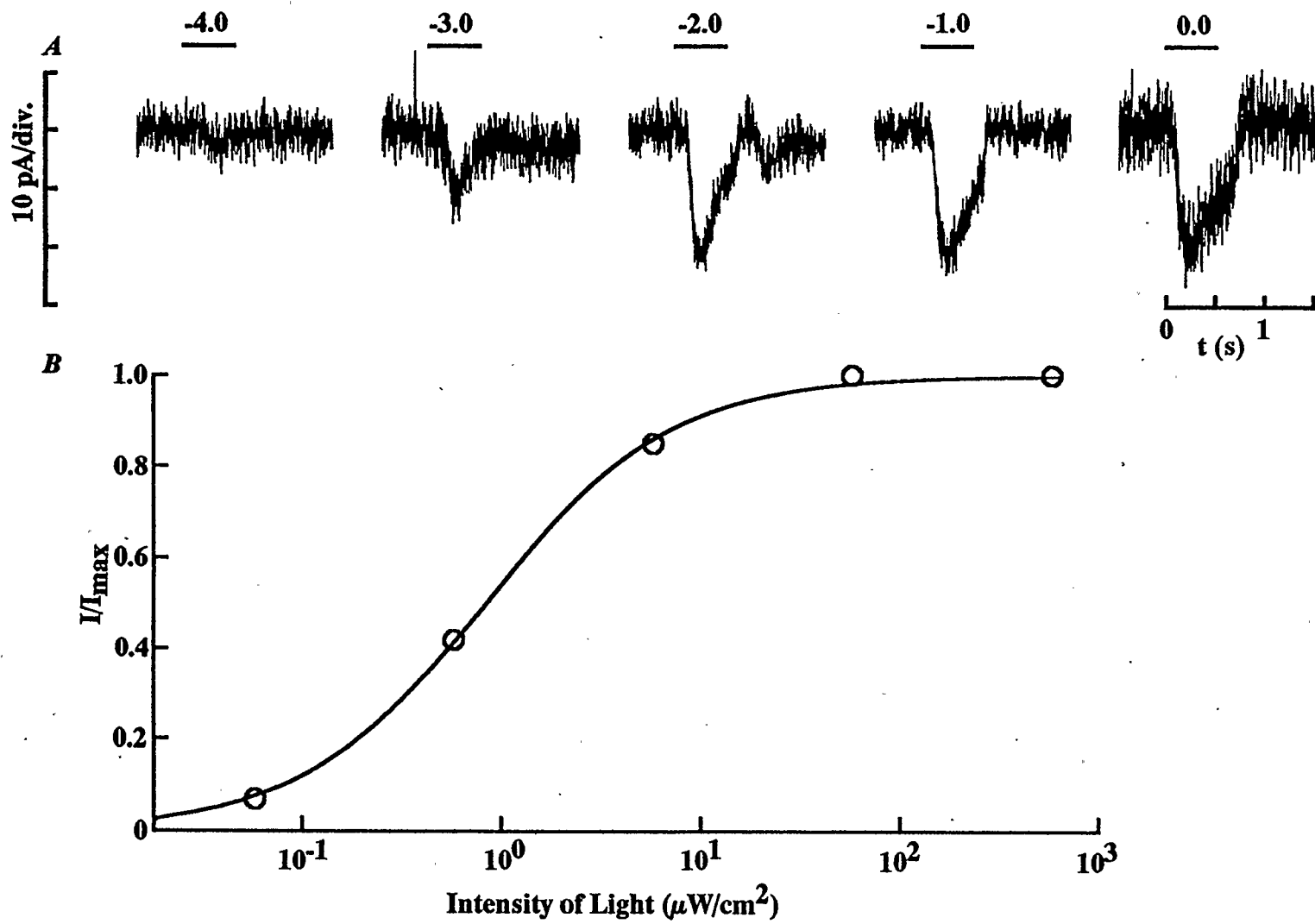


Figure 15.

3.2.1.3 Conclusion

Second order horizontal cells and ON-bipolar cells receive inputs from cones and rods. They respond with hyperpolarization (horizontal cell) and depolarization (ON-bipolar cell) with the size of their responses dependent upon the intensity of light falling on the photoreceptors.

3.2.2 pH Modulation Of Synaptic Transmission

External pH was changed to determine the effects on synaptic transmission to postsynaptic horizontal cells and bipolar cells. Light-elicited postsynaptic currents of horizontal cells at different pH's were compared to a control pH_O of 7.60. Acidification of pH_O to 7.31 reduced postsynaptic standing inward dark current and consequently reduced the light-suppressible current (Figure 16). pH_O 6.94 abolished standing inward dark current and light-suppressible current. The effect at pH_O 6.94 was mimicked by addition of 100 μM Cd²⁺ to the bath presumably via block of presynaptic Ca channels (Barnes & Hille, 1989), which abolished postsynaptic responses. Alkalinization of the external solution to pH_O 7.83 increased standing inward current five-fold and resulted in a larger light response.

3.2.2.1 Exponential Dependence Of Postsynaptic Currents On pH_O

The amount of light-suppressed current during the light step (squares; rod and cone input together) and after the light step (triangles; rod tail input) was measured in different pH_O's and normalized to pH_O 7.60. The data were fit with an exponential relation described by $I = \exp((4.36 \text{pH}) - 33)$ (Figure 17A). When plotted semi-logarithmically, the function is a straight line that exhibits an e-fold increase in current per 0.23 (1/4.36) pH unit between pH_O 7 and 8 (Figure 17B).

Figure 16. Modulation of postsynaptic horizontal cell currents by changes of extracellular pH. 60 pA of inward dark current was suppressed during a bright step ($58 \mu\text{W}/\text{cm}^2$) of light at pH 7.60. After the light step, 43 pA of current was suppressed. Changing bath pH to 7.83 increased standing inward current such that a light step suppressed 188 pA of current. Changing bath pH to 7.31 or 6.94 reduced or abolished, respectively, standing inward current and therefore reduced the amount of light suppressible current. Superfusion of $100 \mu\text{M Cd}^{2+}$ at pH 7.60 also abolished standing inward current. All effects were reversible. Duration of light step at each pH and during the Cd^{2+} experiment was 500 ms. Holding potential, -60 mV. Standard bath solution, pH 7.60; Na-K pipette solution, pH 7.20. Modified from Merchant and Barnes, 1992 and Barnes, Merchant, and Mahmud, submitted.

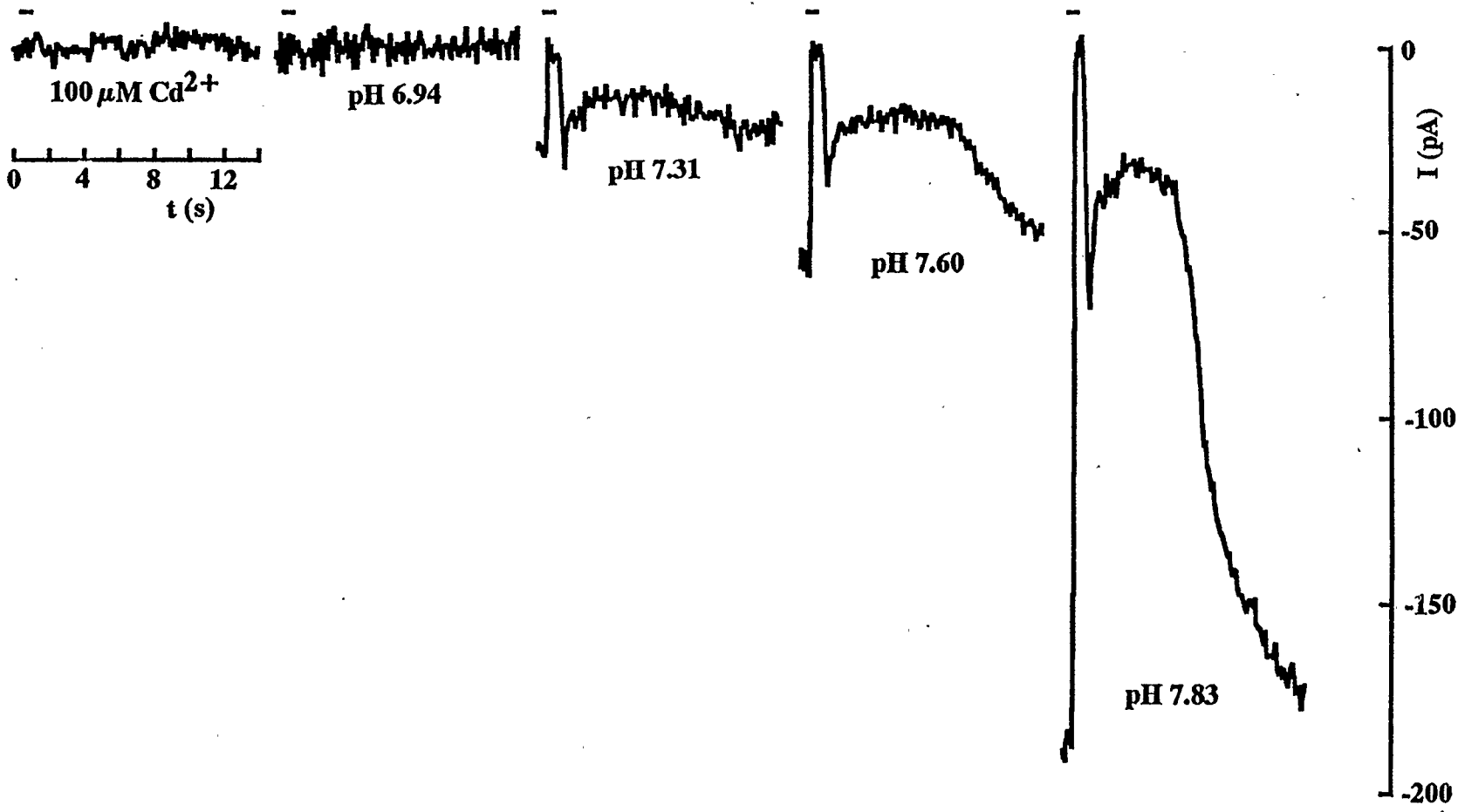
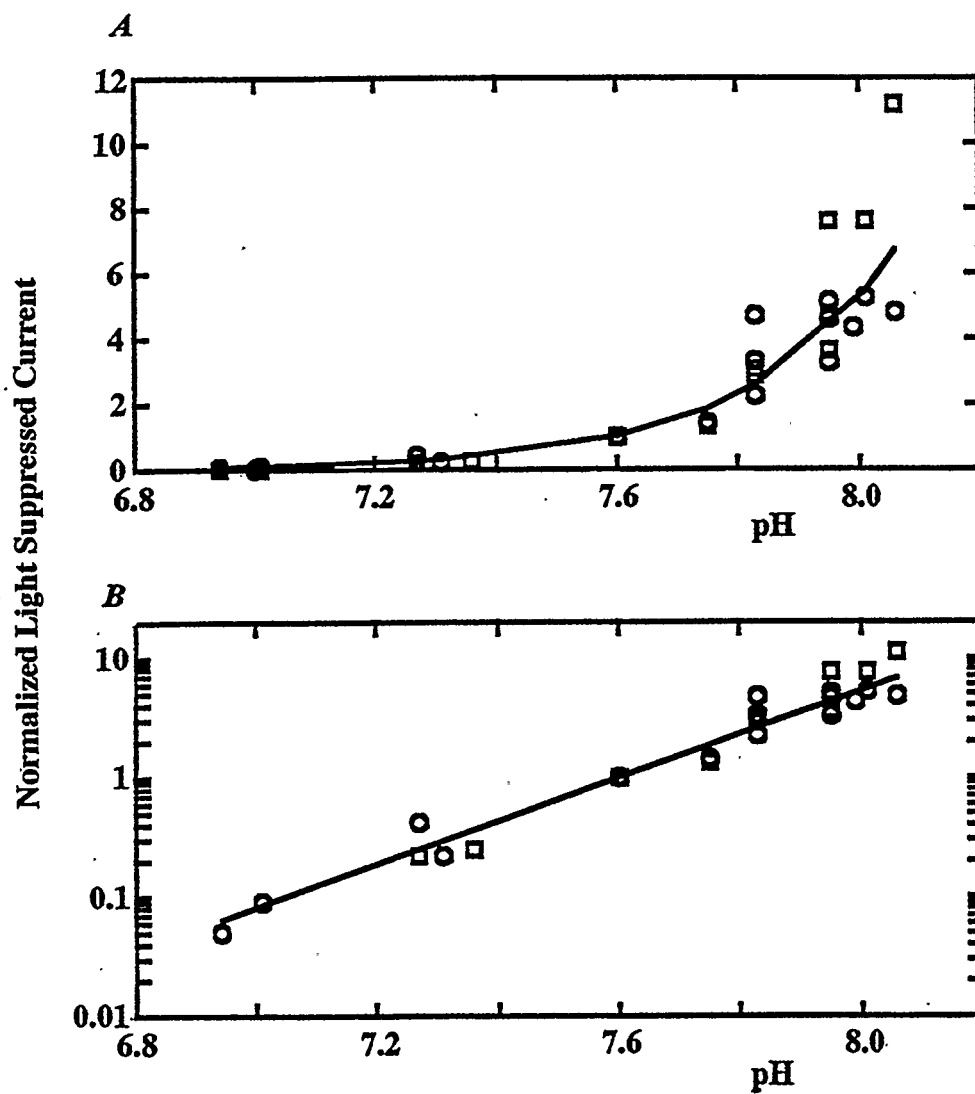


Figure 16.

Figure 17. Exponential dependence of postsynaptic current on pH. *A.* Suppression of current during the light step (triangles; rod and cone input) and after the light step (squares; rod input only) were measured in 5 horizontal cells relative to pH 7.60 and normalized. The least-squares fitted solid line is given by $I = \exp(4.36 \times pH - 33)$. *B.* Semi-logarithmic plot of the data in *A.* The best fit line in *A* was plotted semi-logarithmically. Modified from Merchant and Barnes, 1992 and Barnes, Merchant, and Mahmud, submitted.

*Figure 17.*

Postsynaptic ON-bipolar cell currents were also modulated by pH_O . Light produced a 20 pA inward current in the cell in Figure 18A at pH 7.60. Changing pH_O to 7.99 increased the light-elicited current to 100 pA (Figure 18B). This increase fits on the curve measured in Figure 17 for horizontal cell pH_O sensitivity. In the dark, ON-bipolar cells are hyperpolarized via APB receptor mediated suppression of cGMP-activated channels (Nawy & Jahr, 1990, 1991; Shiells & Falk, 1992a,b). Horizontal cells have been shown to be depolarized in the dark via non-NMDA receptors, specifically, kainate, quisqualate, and AMPA receptors (Yang & Wu, 1991; Wilson, Gleason, & Gilbertson, 1991; Slaughter & Miller, 1981, 1983b, 1985). It is possible that pH_O is affecting these postsynaptic receptors. pH_O affects both horizontal cells and ON-bipolar cells in a similar manner. However, non-NMDA receptor currents have been shown to be little affected by changes of pH_O in the range of pH_O 6.8 to 8 (Tang, Dichter, & Morad, 1990; Christensen & Hida, 1990; Traynelis & Cull-Candy, 1990). Perhaps protons are acting at the presynaptic membrane. As shown in Figure 6 and by Barnes and Bui (1990) and Mahmud and Barnes (1992), changes of pH_O modulate Ca channels of photoreceptors. Thus pH_O may be modulating postsynaptic currents via modulation of presynaptic Ca channels that may be responsible for synaptic transfer.

3.2.2.2 Shifts Of The Synaptic Transfer Function

Using microelectrodes in tiger salamander retina, Attwell *et al.* (1987) simultaneously recorded rod and horizontal cell voltage as a function of rod voltage. These values were then used to generate a synaptic transfer function that was fit with an exponential relation (Figure 19A). If this function underlies the action of Ca channels at the synapse then lateral shifts of the synaptic transfer function could account for the exponential dependence of postsynaptic currents on pH_O . The

Figure 18. Modulation of postsynaptic ON-bipolar cell currents by changes of extracellular pH. A step of light ($18 \mu\text{W}/\text{cm}^2$, duration was 500 ms) elicited a 60 pA inward current at pH 7.60 in the cell held at -60 mV. This response was increased 5-fold when extracellular bath pH was changed to 7.99. Standard bath solution, pH 7.60; Na-K pipette solution, pH 7.20. Modified from Merchant and Barnes, 1992 and Barnes, Merchant, and Mahmud, submitted.

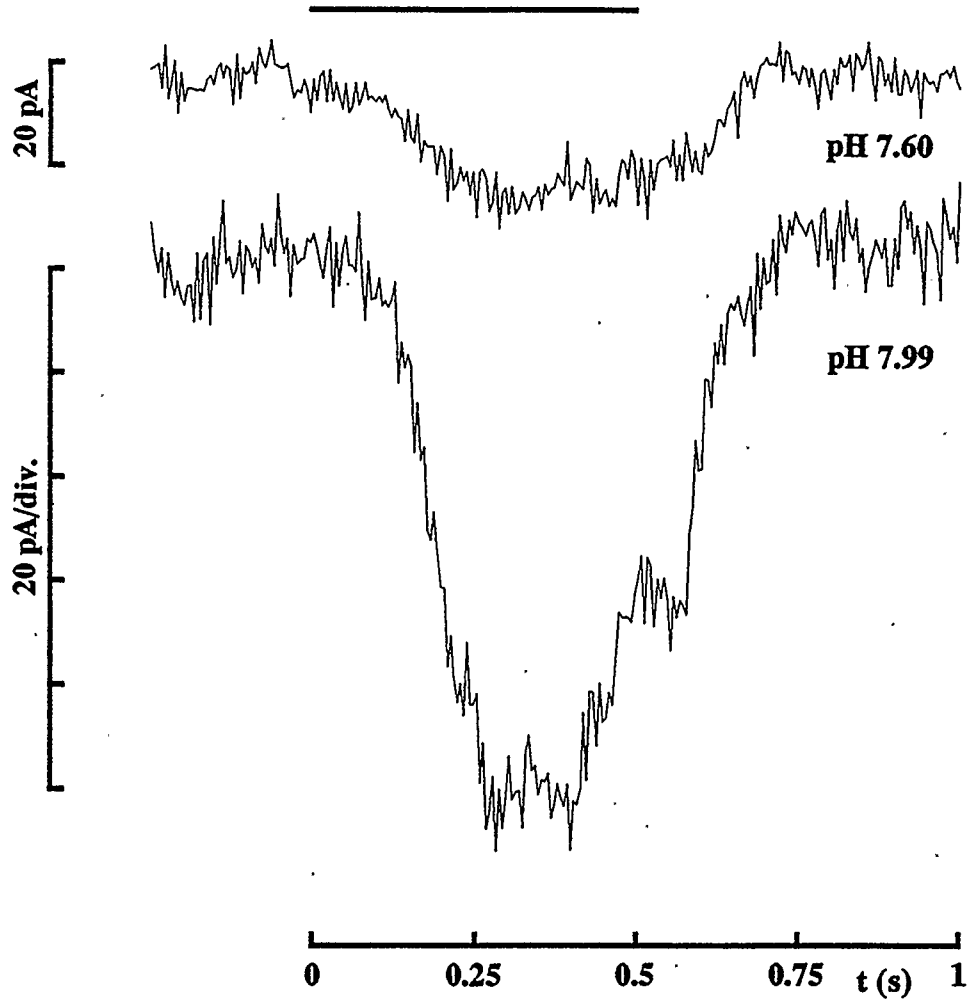


Figure 18.

Figure 19. Lateral shifts of the synaptic transfer function. *A.* Synaptic transfer function of the photoreceptor output synapse described by $V_H = A \{ \exp (V_R/k) - 1 \}$ where $A = 39$ mV, $k = 2.1$ mV and V_H and V_R are light-induced changes in membrane potential of horizontal cells and rod photoreceptors, relative to their dark resting potentials of -32 mV and -40 mV, at pH 7.60. Modified from Attwell, Borges, Wu, & Wilson, 1987. *B.* The function in A was reformulated to give responses in terms of postsynaptic current (V_H become I_{post} and $A = -61$ pA to match the response of Figure 16; for graphing, inward (negative) current was plotted upwards). The relation became $I_{post} = -61 \text{ pA} \{ \exp (V_R/2.1) - 1 \}$. The exponential relation was then shifted laterally in the positive direction by 3.3 mV and 7.9 mV for pH 7.31 and 6.94, respectively, and negative by 2.4 mV for pH 7.83, which are the values given by the shifts of the curve describing Ca channel gating from Barnes & Bui (1989) and Mahmud and Barnes (1992). Photoreceptors respond to bright light by hyperpolarizing from their dark potential (V_{dark} , near -40 mV) to potentials at least 10 mV more negative (V_{light} , -50 mV or beyond). *Inset.* The expected changes in synaptic current in response to bright light at the different pH values were estimated (vertical lines at right of *B*), normalized, and plotted (circles) with the exponential function (solid line) from Figure 17. Modified from Merchant and Barnes, 1992 and Barnes, Merchant, and Mahmud, submitted.

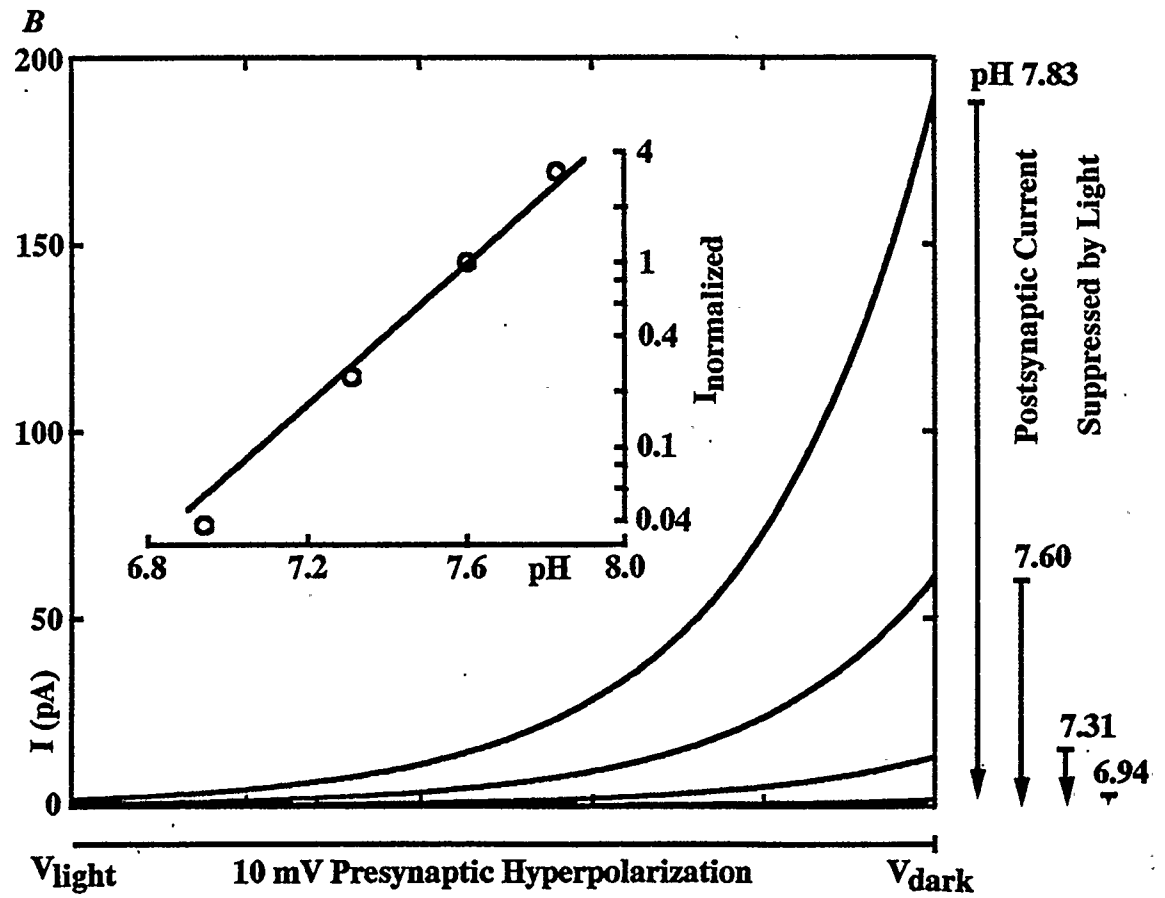
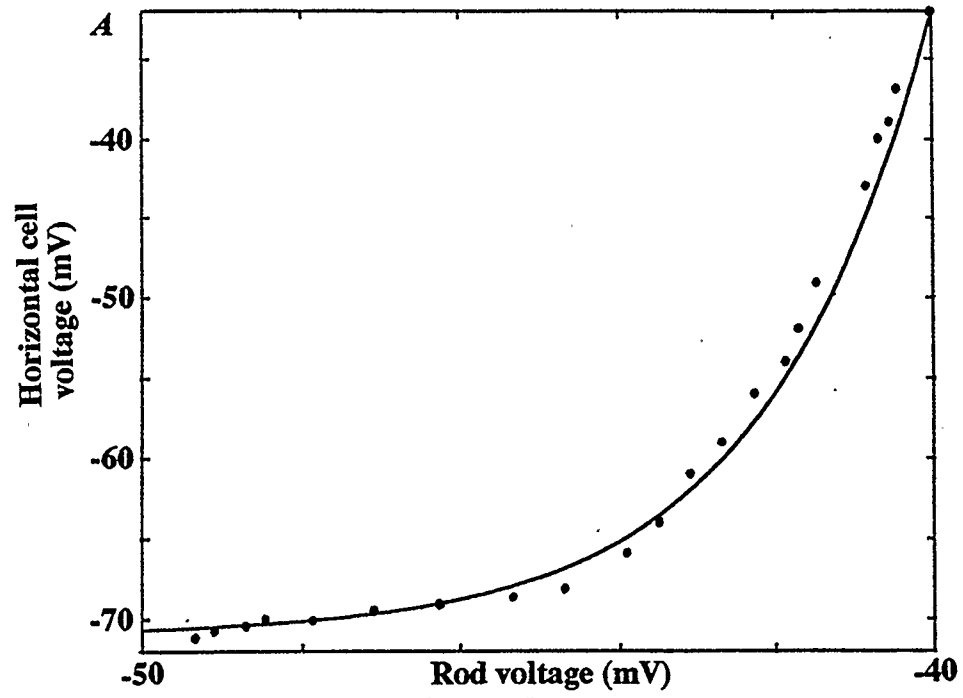


Figure 19.

synaptic transfer function described by Attwell *et al.* (1987) was $V_H = A \{ \exp(V_R/k) - 1 \}$ (where $A = 39$ mV, $k = 2.1$ mV and V_H and V_R are light-induced changes in membrane potential of horizontal cells and rod photoreceptors, relative to their dark resting potentials of -32 mV and -40 mV, respectively, at pH_O 7.6). This function was reformulated to give responses in terms of postsynaptic current such that V_H became I_{post} and $A = -61$ pA to match the response at pH 7.60 in Figure 16 above. The synaptic transfer function expressed in terms of postsynaptic current would become $I_{post} = -61 \text{ pA} \{ \exp(V_R/2.1) - 1 \}$. Inward (negative) current is plotted upwards to match the direction of Attwell *et al.*'s (1987) synaptic transfer function. The relation was shifted laterally along the presynaptic voltage axis by amounts prescribed by the shifts in Ca channel activation described by Barnes and Bui (1989) and Mahmud and Barnes (1992). For pH_O 7.31 and 6.94 the function was shifted in the positive direction by 3.3 mV and 7.9 mV, respectively (Figure 19B). The function was shifted negative by 2.4 mV for pH_O 7.83 (Figure 19B).

The expected *changes* in postsynaptic current due to bright illumination at each pH are illustrated as vertical lines at the right in Figure 19B. These changes were normalized and plotted (circles) in the inset. They fall close to the relation describing pH-dependence of postsynaptic current (solid line) measured in Figure 17B above, suggesting that pH-induced shifts of the synaptic transfer function could account for transmission modulation.

3.2.3.3 Conclusion

Postsynaptic horizontal and ON-bipolar currents are modulated by pH_O in an exponential fashion in the range of pH_O 7 to 8. Lateral shifts of the synaptic transfer function, relating pre- and postsynaptic voltage, by amounts prescribed by pH_O dependent shifts in Ca channel activation midpoint can account for these findings.

3.3 Feedback to cones

3.3.1 Methods for Generating the Feedback Signal

Simultaneous microelectrode recordings from rod and cone photoreceptors previously showed that hyperpolarizing current injected into a rod induced hyperpolarization in a neighboring cone (Attwell *et al.*, 1983). Termination of the hyperpolarizing current injected into the rod resulted in repolarization of the cone. In addition, approximately 50-100 ms after the repolarization of the cone, a transient hyperpolarization was recorded in the cone. Furthermore, Attwell *et al.* (1983) found that if the microelectrode was left in the cone for a long time (the cell responded very weakly to light under these conditions) or if the outer segment of the cone was damaged, only the transient hyperpolarization at the end of the current injection was recorded. This transient hyperpolarization in the cone is the feedback signal that was simultaneously recorded as an inverted (depolarizing) signal of a horizontal cell (Attwell *et al.*, 1987). This sudden depolarization in the horizontal cell at the offset of light or upon repolarization is probably via a regenerative depolarization dependent on calcium which has been recorded in skate horizontal cells (Lasater & Dowling, 1982; Lasater, Dowling, & Ripps, 1984) and catfish horizontal cells (Johnston & Lam, 1981).

Several techniques were used to generate the transient feedback signal that stands above noise. The goal of the following manipulations was to generate transient depolarizations in horizontal cells that will feed back to cones.

3.3.1.1 The Headless Cone

Retinal slices were made as described in section 2.1 above but under infrared illumination. Under the microscope, using an infrared sensitive TV camera, the outer segment of the cone was sucked off to render it unresponsive to light (similar to Attwell *et al.*, 1983). This procedure was required because the cone

feedback signal together with the light response would otherwise be superimposed upon each other. The photoreceptor remained healthy without the outer segment. Furthermore, this "headless" cone preparation served as the perfect annulus for which broad field illumination was used to drive the synaptic input (electrical coupling is weak between salamander cones but stronger between salamander horizontal cells (Attwell, Werblin, & Wu, 1984)). It is possible that incomplete removal of the outer segment might have obscured the feedback signal. The reversal potential of the feedback response was measured using this technique (see section 3.3.2.1).

3.3.1.2 Driving The Rod Network Using TEA

Retinal slices were made under normal illumination and a cone was whole-cell patch clamped. Superfusion of 20 mM TEA in normal ringer solution should have caused rods to depolarize and possibly spike regeneratively (via calcium). This signal would then be synchronized in the rod network and would drive horizontal cells with transient depolarizations that will be fed back onto the cone that was being recorded from (Barnes & Werblin, unpublished observations). This technique had the added advantage that blockage of cone noisy outwardly rectifying K channels by 20 mM TEA facilitated the analysis of the feedback signal at depolarized potentials.

3.3.1.3 Pumping Up The Horizontal Cell

Puffing an agent to depolarize horizontal cells directly may help to avoid the unreliability of the techniques above. Once again, retinal slices were made under normal illumination and a cone was patch clamped. A puffer pipette positioned approximately 50 - 100 μm away from the cell that was recorded from puffed out 2 mM L-Glutamate (in the presence of 20 mM TEA in normal ringer solution) onto horizontal cells. Glutamate directly depolarizes horizontal cells and causes them to

spike in the presence of TEA. These spikes were expected to propagate through the horizontal cell network (which is coupled electrically) and feed back onto the cone. Other agents such as L-aspartate (Ishida & Fain, 1981) or kainate that act at the excitatory amino acid receptors on horizontal cells may have increased the chances of reliably recording the feedback signal but were not tested.

3.3.1.4 Conclusion

It was determined that the feedback response was best observed using the headless cone technique. Techniques 2 and 3 gave unreliable and unresolvable signals.

3.3.2 The Feedback Response

As described in section 1.4.3, the feedback pathway from horizontal cells to cones probably involves the release of GABA from horizontal cells acting at GABA_A receptors on cones (Kaneko & Tachibana, 1986; Wu, 1991). Figure 20A shows the light response of a light-adapted cone photoreceptor that had an intact outer segment. Standing inward current in the dark is suppressed by a 500 ms light step ($58 \mu\text{W}/\text{cm}^2$). At the end of the light step, a large transient inward current is recorded before the current level returns to baseline dark current (see below). Feedback from horizontal cells continuously influences cone photoreceptors. However this influence is difficult to resolve if light-elicited currents are dominating the response. The headless cone technique allows for resolution of the feedback signal during and after the light step.

The cone in Figure 20B had its outer segment removed. A light step generated a response waveform that was smaller but similar to the waveform in A. Using the scheme describing the involvement of the GABA_A receptor/Cl channel in section 1.4.3, the response in Figure 20B can be analyzed as follows. In the dark, horizontal cells are depolarized and continuously release GABA onto

Figure 20. Generation and resolution of the feedback signal in cones. *A.* Light-elicited response and feedback transient in one member of a double cone voltage-clamped at -60 mV. The outer segment in this cell was not removed. Average of 5 responses. *B.* Feedback signal from a single cone clamped at -60 mV that has had its outer segment removed. Average of 10 responses. *C.* Current clamp of a single cone that had a resting potential of -39 mV. The outer segment was attached. Light elicited a 10 mV hyperpolarization and an overshoot at the end of the step. No averaging. In all cases, standard bath solution, pH 7.60; Na-K pipette solution, pH 7.20. Intensity of light stimulus, $58 \mu\text{W}/\text{cm}^2$, duration 500 ms.

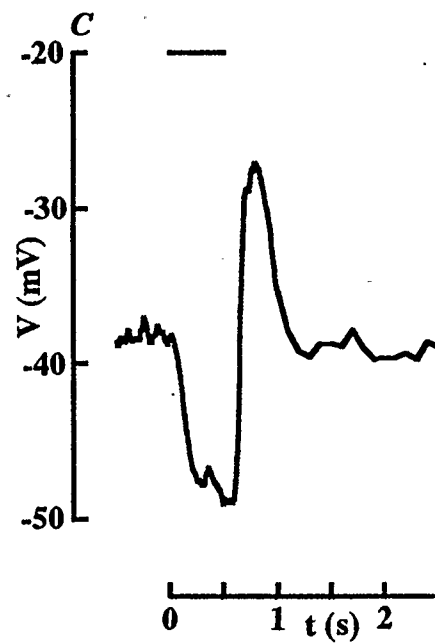
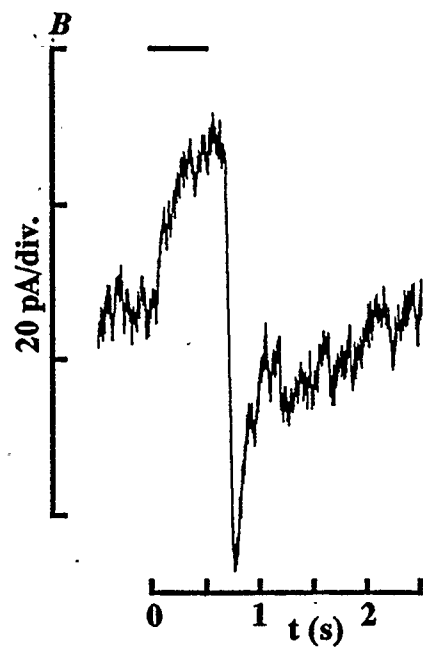
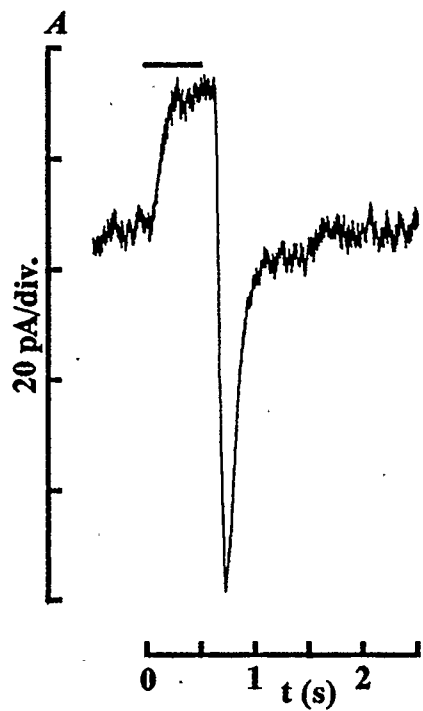


Figure 20.

photoreceptors. Therefore, GABA_A receptor/Cl channels in cones remain open. If the chloride equilibrium potential in cones is near 0 mV, as it might be with 107 mM Cl⁻ in the pipette, then Cl⁻ conductance might be expected to depolarize the cone (i.e. a standing inward current). Light hyperpolarizes other photoreceptors with intact outer segments and consequently hyperpolarizes horizontal cells. Horizontal cell hyperpolarization may result in reduction of GABA release onto cones, closure of GABA_A receptor/Cl channels, and cone hyperpolarization. This is represented in Figure 20B during the light step as a reduction of inward current. After the light step, a regenerative depolarizing response in horizontal cells (Johnston & Lam, 1981; Lasater & Dowling, 1982; Lasater, Dowling, & Ripps, 1984) is reflected as a transient inward current in the cone.

Figure 20C shows the transient feedback signal in a cone under current clamp with an intact outer segment. It was possible to record the feedback transient with or without the outer segment. Notice that the polarity of the feedback response (inward current or transient depolarization) was opposite in polarity to that recorded by Attwell *et al.* (1983). This is a function of the chloride equilibrium potential (as described above; also see section 4.3.1).

3.3.2.1 Reversal Potential Of The Feedback Response

The feedback response was measured at various membrane potentials from a cone without an outer segment. Figure 21A shows that at a holding potential of -60 mV, the transient portion of the feedback signal was readily observable after a 1500 ms light step. Holding the cell at -40 mV resulted in some outward current and in a reduction of the feedback signal. Further depolarizations generated larger outward currents and reduction of the feedback signal until it was not distinguishable from the outward currents. Current at the peak of the feedback

Figure 21. Reversal potential of the feedback response in a headless cone. *A.* A single cone was held at different holding potentials to determine the reversal potential of the feedback signal. The outer segment was removed in this cell. At a holding potential of -60 mV a 1500 ms light stimulus elicited a small outward current and the feedback transient. Holding the cell at more depolarized potentials reduced the feedback transient until it was not resolvable from the background potassium current. Standard bath solution, pH 7.60; Na-K pipette solution, pH 7.20. *B.* The peak current during the feedback transient at -60, -40, and -20 mV was measured and plotted against holding potential (circles). The least-squares fit was described by $I = 3.793085 + 1.888699 \times \text{voltage}$.

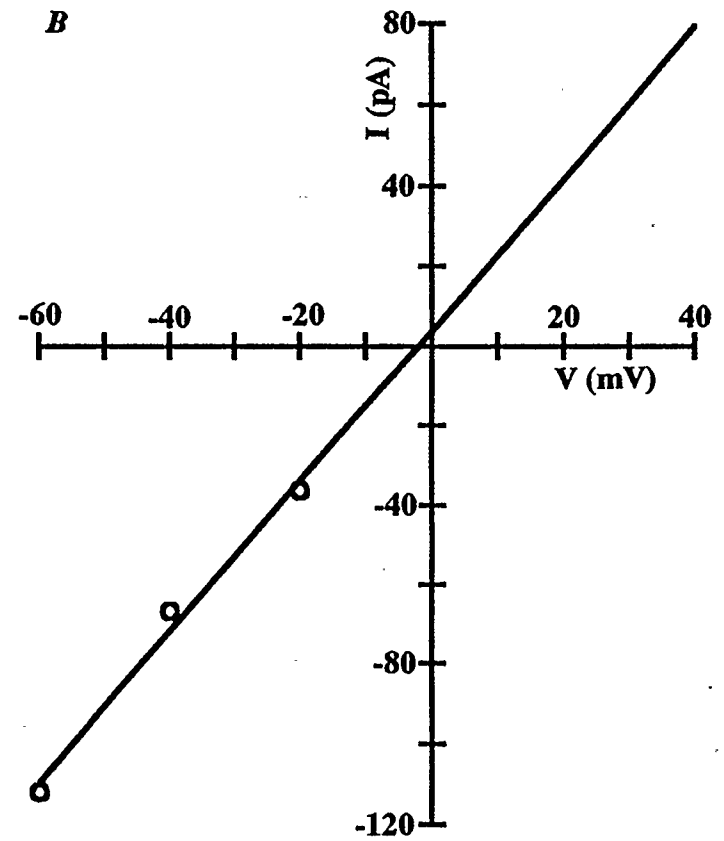
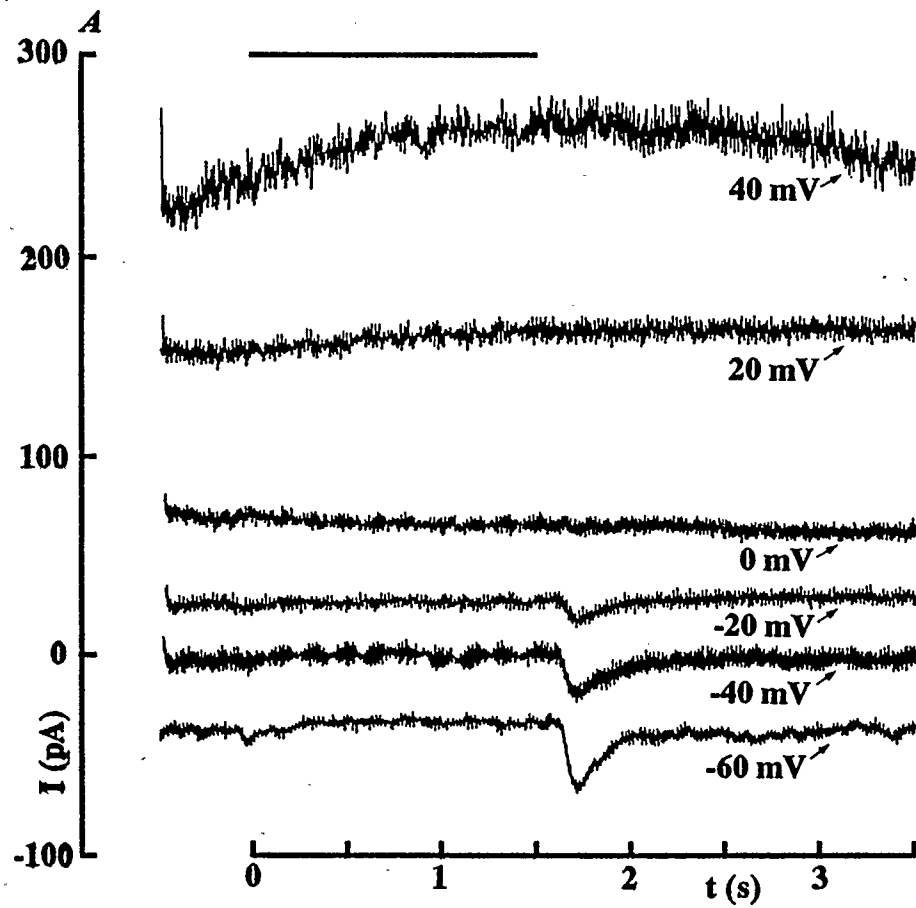


Figure 21.

signal at -60, -40, and -20 mV was plotted against voltage in Figure 21B. If only the peak feedback current values between -60 mV and -20 mV are taken, then a best fit line through these points shows a reversal potential of the feedback response near 00 mV. This suggests that the chloride equilibrium potential is near 0 mV in this cell, more positive than that recorded by Attwell *et al.* (1983) and Skryzpek & Werblin (1983). The feedback signal did not reverse at positive potentials. It is possible that outward currents mask the feedback signal.

3.3.2.2 Modulation Of Ion Channels

GABA, the proposed feedback transmitter was superfused onto cone photoreceptors in the light to determine its effects. Whole-cell recordings were made from a cone in normal bath solution (Figure 22A, upper set). Superfusion of 100 μ M GABA (middle set) seemed to eliminate outward calcium-activated potassium currents. Upon washout of GABA (lower set), $I_{K(Ca)}$ did not recover. This is further demonstrated in the I-V relations in Figure 22B showing current before (circles), during (squares), and after (triangles) application of 100 μ M GABA.

GABA also seemed to reduce calcium-activated chloride current. Figure 23A shows I-V relations from a cone before (circles), during (squares), and after (triangles) application of 100 μ M GABA. Inward current was reduced and this effect was not reversible. This effect was additionally demonstrated in Figure 23B. I-V relations of calcium-activated chloride tail currents 50 ms after the preceding voltage step show that they are irreversibly reduced. The time course of control, drug application, and washout was relatively short (minutes). Furthermore, under normal conditions $I_{Cl(Ca)}$ and $I_{K(Ca)}$ remained relatively robust in cones in slices over a similar time course and superfusion paradigms.

Figure 22. Modulation of $I_{K(Ca)}$ in cones by 100 μ M GABA. *A.* One member of a double cone was held at a potential of -50 mV and depolarized in 10 mV increments to potentials ranging from -40 to 130 mV. These currents are shown under control (upper), in 100 μ M GABA (middle), and wash conditions (lower). Standard bath solution, pH 7.60; CsCl pipette solution, pH 7.20. *B.* I-V relation of $I_{K(Ca)}$ recorded in *A.* Superfusion of 100 μ M GABA onto the cone irreversibly reduced $I_{K(Ca)}$. Circles = control, squares = 100 μ M GABA, and triangles = wash.

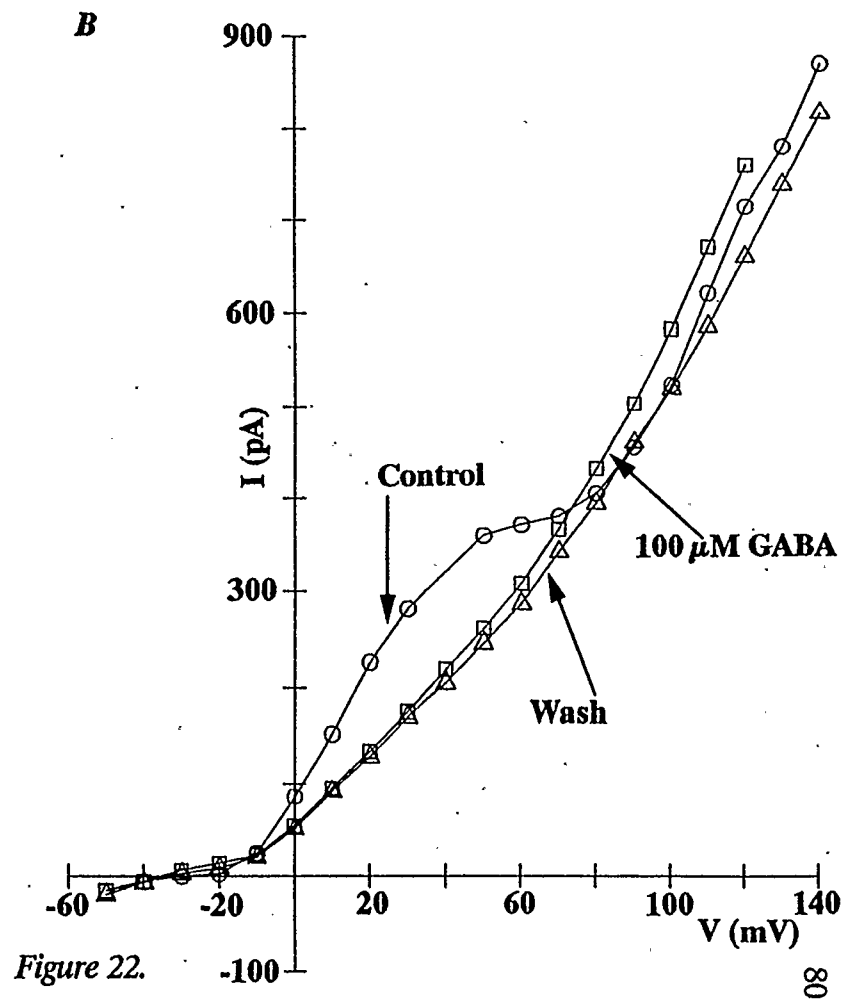
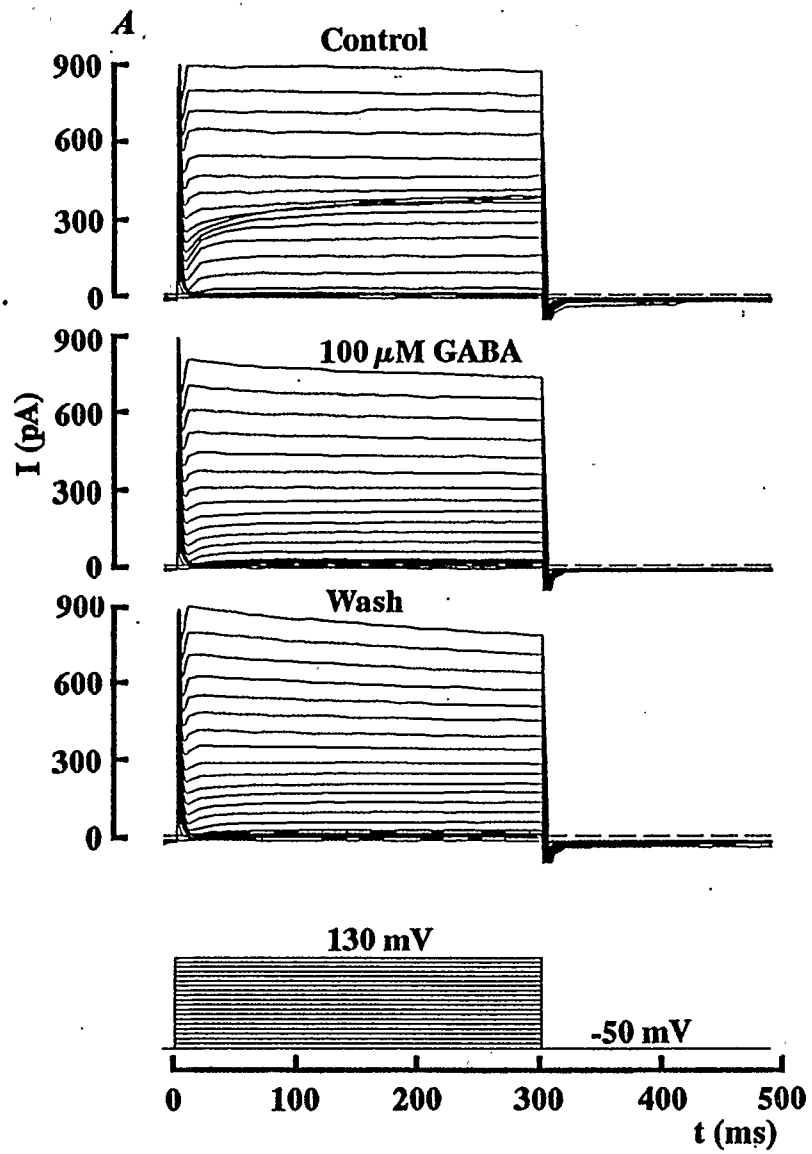


Figure 22.

Figure 23. Modulation of $I_{Cl(Ca)}$ in cones by 100 μ M GABA. *A.* I-V relation of $I_{Cl(Ca)}$ recorded by depolarizing a single cone from a holding potential of -50 mV in 10 mV increments. Superfusion of 100 μ M GABA irreversibly reduced $I_{Cl(Ca)}$. *B.* $I_{Cl(Ca)}$ tail currents measured 50 ms after the depolarizing step command show a similar reduction in the presence of 100 μ M GABA. Circles=control, squares=100 μ M GABA, and triangles=wash. In both cases, standard bath solution, pH 7.60; CsCl pipette solution, pH 7.20.

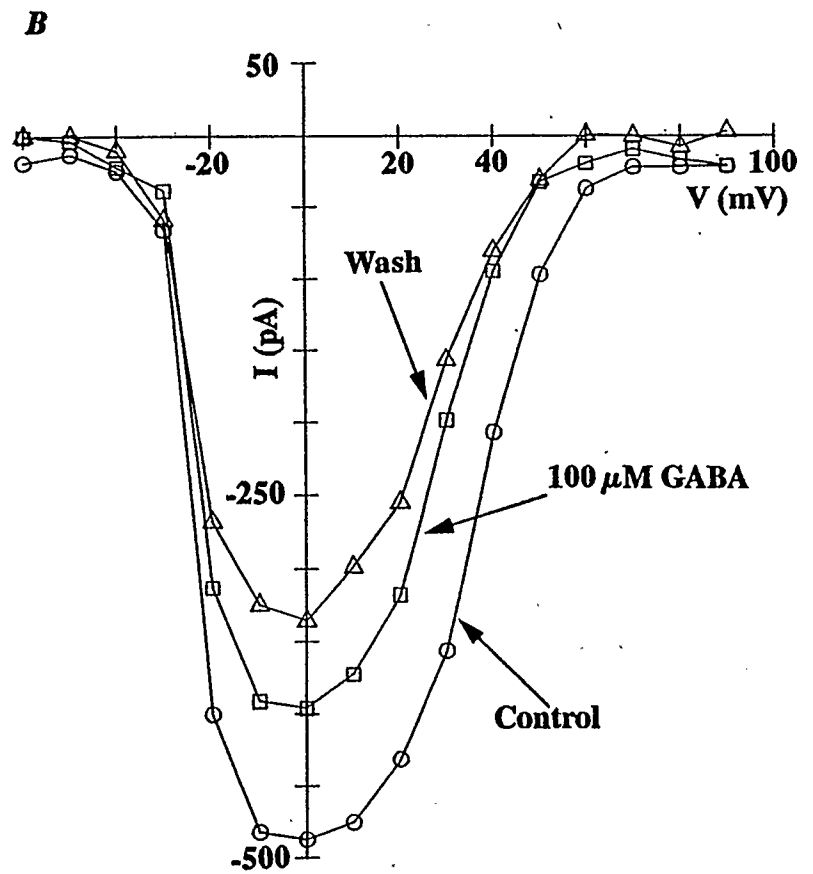
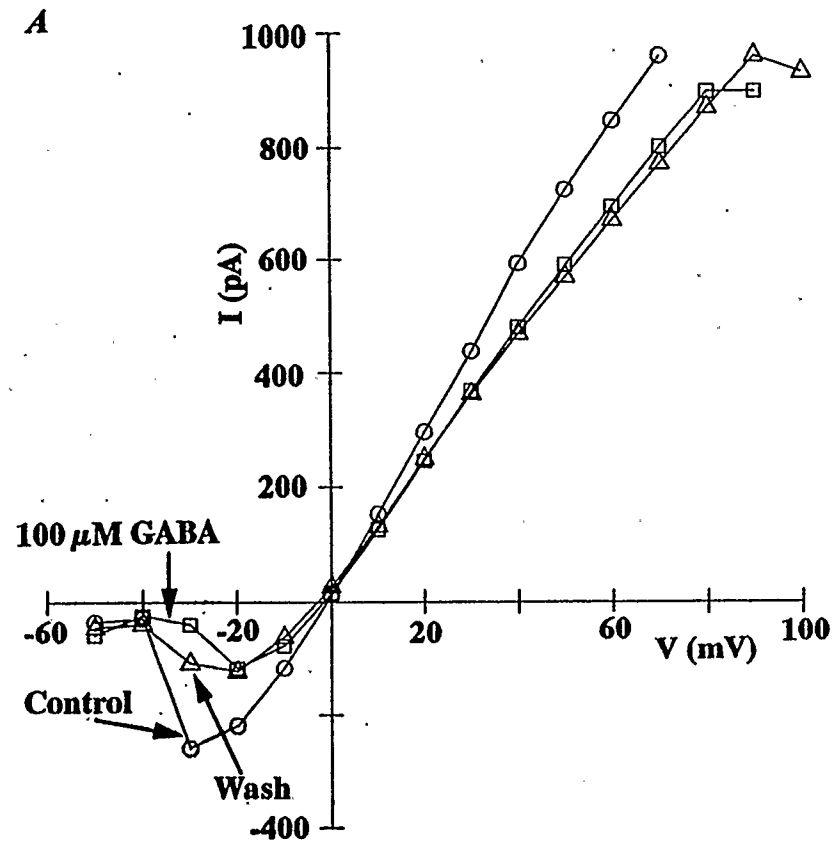


Figure 23.

3.3.2.3 Conclusion

Superfusion of 100 μM GABA onto cones has shown that $I_{\text{K}}(\text{Ca})$ and $I_{\text{Cl}}(\text{Ca})$ may be modulated, possibly via an underlying modulation of Ca channels. Both currents were reduced but this effect was irreversible and was only recorded in six cones studied with GABA. The extrapolated reversal of the feedback response near 0 mV suggests that the GABA_A receptor/chloride channel may be involved.

CHAPTER 4

DISCUSSION

This work examines the synaptic interactions in the outer plexiform layer of the tiger salamander retina. It was determined that extracellular pH modulates the photoreceptor output synapse probably by modulating presynaptic Ca channels of cones. Synaptic inputs to these cones are probably mediated via GABA mediated feedback from horizontal cells. In order to analyze these effects, the properties of the cone photoreceptor were measured.

4.1 The Cone Photoreceptor

4.1.1 Coupling Between The Cell Body And Telodendrites Is Good Bidirectionally

The cone photoreceptor is a unique cell with many properties that help its function. On average, tiger salamander cones are 10-15 μm in diameter and have about 5 telodendrites extending from their pedicles. Passive electrical properties such as capacitance and input resistance were measured and used in the cell simulation program *Manuel*. It was determined that bidirectional communication between the cell body and its telodendrites was very good with values being $V_{\text{telo}} = .99 V_{\text{cb}}$ and $V_{\text{cb}} = .88 V_{\text{telo}}$. Previous results of have also shown good bidirectional communication between walleye cone cell bodies and telodendrites (Kraft & Burkhardt, 1986).

It seems that signals arising at the cell body are effectively transmitted to the telodendrite. Suppose that the cell body signal is large. Although there may be shunting of the signal by the morphological properties (beaded nature) of the telodendrites, this shunt may be insignificant compared to the signal generated in the large cell body area. A similar sort of morphological shunting mechanism is

present for signals arising at the telodendrite. It is possible that signals arising at the telodendrite are small and undergo a similar shunt. This would reduce the magnitude of the signal. Furthermore, this signal at the cell body might be attenuated by large conductances at the cell body.

Changes in properties such as telodendrite diameter (axial resistance), telodendrite calcium channel density, and a strong shunt at the cell body all failed to completely uncouple the cell body and telodendrite. Only telodendrite diameter (using a $0.3 \mu\text{m}$ telodendrite) was effective in reducing coupling below 50%. However, electron microscopy (Lasansky, 1971, 1973) has shown that these telodendrites have a diameter of about $1 \mu\text{m}$. Simulations using the $1 \mu\text{m}$ diameter telodendrite gave high values for coupling ratios. Therefore, coupling below 50% may be the exception in that it doesn't correspond to the morphological evidence.

It is possible that under some conditions, in some animals, uncoupling may occur, but given the range of parameters tested here, such uncoupling is unlikely in salamander cones. If telodendrites serve as sites of lateral signal interaction then communication to the cell body would not be hampered by the dynamic properties of the telodendrite itself.

4.1.2 Ionic Currents Shape The Responses Of Cones

Ionic currents in the inner segment of cones include calcium, and calcium-activated currents, two potassium currents, and a non-selective cation current. These currents measured in retinal slices corresponded well with currents measured in isolated cells (Barnes & Hille, 1989). It was observed that the calcium-activated chloride current, $I_{\text{Cl}}(\text{Ca})$, was larger in amplitude when measured in slices. It is possible that some of these channels are present either at the cone pedicle or on the telodendrites. During enzymatic cell isolation, the pedicle and processes may be damaged such that channels are no longer viable and consequently currents are

not measured. It was found that enzymatically isolated cones had an average of 10 pF less capacitance than mechanically isolated cells (Barnes & Hille, 1989). If slices are considered as a "mechanically isolated" preparation, then they may be better assays for the study of these ion channels.

Ca channels of cone photoreceptors were shown to be sensitive to extracellular pH. It was determined that cones in retinal slices exhibit a 10-12 mV shift in midpoint of Ca channel activation in the pH range of 7 to 8. This result is consistent with the result found in isolated cone (Barnes & Bui, 1991) and rods (Mahmud & Barnes, 1992). Isolated cells showed a 10-15 mV shift in the midpoint of Ca channel activation in the same pH range. This action may be through alteration of gating and permeation via generation of a surface charge screening effect that may reduce the local calcium concentration at the mouth of the channel and by proton block of the channel (Barnes & Bui, 1991). However, the local extracellular concentration of Ca (about 3 mM) is much more than the local proton concentration ($10^{-7.6}$ M). A small change in the proton concentration (e.g. from $10^{-7.6}$ to $10^{-7.8}$) may be insignificant in terms of surface charge screening. It is possible that protons are acting at a specific site on or in the channel to produce these changes.

These properties of the ionic currents of cones in retinal slices play an important role in the function of the inner segment where most of these channels are found. They serve to shape the light-elicited currents of the outer segment.

4.1.3 Cones Respond Maximally To Bright Light Of 600 To 650 nm.

Bright light ($580 \mu\text{W}/\text{cm}^2$) reduced a standing inward current in cones in retinal slices. This response was between 10-40 pA in amplitude and was similar to previous suction electrode recordings in tiger salamander (Schnapf & McBurney, 1980). Cone responses increased with increases in the intensity of illumination. It

was not possible to determine whether the responses were facilitated by the illumination of neighbouring cones (Baylor *et al.*, 1971) because broad field illumination, used here, polarized all cones equally.

In salamander, cones are red sensitive ($\lambda_{\max}=620$ nm) and rods are green sensitive ($\lambda_{\max}=520$ nm; Attwell *et al.*, 1983). Single (Attwell, Werblin, & Wilson, 1982) and double cones (Attwell, Wilson, & Wu, 1984) have been shown to be maximally responsive to wavelengths of light between 600 and 620 nm. Spectral response measured in this study gave similar results. Cones in retinal slices under voltage clamp were maximally responsive to bright light of wavelengths between 600 and 650 nm. The maximum responsiveness of cones to one narrow band of wavelength simplified the analysis of light-elicited currents. Contributions from colour-opponent processing (if present) in the OPL were negligible.

4.2 pH_o And Synaptic Transmission

External factors can modulate the activity of cone photoreceptors to an extent that postsynaptic mechanisms are affected. Extracellular pH has been shown to modify activation of rod and cone Ca channels. If these Ca channels play a role in synaptic transmission to horizontal cells and bipolar cells, then the activity of these second order cells may also be modified.

4.2.1 Postsynaptic Cells Are Modulated By Changes of pH_o

Postsynaptic horizontal cell and ON-bipolar cell currents were modulated by pH_o. Specifically, their light-elicited currents were exponentially dependent on pH_o exhibiting a e-fold increase in current per 0.23 pH unit. Similar results have been found by Kleinschmidt (1991) and Harsanyi and Mangel (1992).

4.2.2 Modulation Of Presynaptic Ca Channels Account For The Exponential Dependence Of Postsynaptic Currents On pH

The site of pH_o action may be pre- or postsynaptic. Cd²⁺ (100 μM) which has been shown to block Ca channels of cones (Barnes & Hille, 1989) also blocked the light-elicited currents of a horizontal cell (Figure 16). Furthermore, horizontal cells and ON-bipolar cells have non-NMDA (Kainate, AMPA) and APB receptors, respectively (see section 1.3.3 above). Increasing pH_o affected both horizontal cells and ON-bipolar cells by increasing the amount of postsynaptic current. It seems unlikely that similar responses to extracellular pH are possible with these differing receptor mechanisms. Also, no changes were observed in the magnitude of glutamate-activated currents (not shown) in horizontal cell in slices over the pH range from 7.60 to 7.95, the range showing the largest changes in light-sensitive synaptic current. Non-NMDA activated currents were negligibly affected by extracellular [H⁺] in the pH range from 6.8 to 8.0 (Tang, Dichter & Morad, 1990; Christensen & Hida, 1990; Traynelis & Cull-Candy, 1990).

It is possible that external pH modified coupling between horizontal cells. Previous studies have shown that lowering intracellular pH lowers gap junction permeability in horizontal cells (Negishi, Teranishi & Kato, 1985) and in amphibian cleavage-stage blastomeres and teleost embryos (Spray, Harris, & Bennett, 1981). Horizontal cells in this work were dialyzed with 10 mM HEPES (pH 7.2), which probably maintained gap junction permeability at a low level (Spray, Harris, & Bennett, 1981). Furthermore, horizontal cells in tiger salamander retina are not tightly coupled to each other such that current changes in neighbouring cells probably do not greatly affect the cell being recorded from. Broad field illumination was used to polarize all cells equally, thus reducing current flow through gap junctions. Also, since the horizontal cell was voltage-clamped, contributions from voltage- and calcium-gated channels in these cells were probably minimized.

The site of pH_O action is probably presynaptic. Possible presynaptic sites include the photoreceptor light-sensitive machinery in the outer segment and the ion channels in the inner segment responsible for synaptic transmission. Properties of the dark current (Liebman, Mueller, & Pugh, 1984), Na-Ca-K exchange (Hodgkin & Nunn, 1987), and aspartate-isolated receptor potential of the electroretinogram (Sillman, Owen, & Fernandez, 1972) are not significantly affected over the range of pH_O having effects on transmission with the time course described here.

Presynaptic Ca channels have been shown to be modulated by extracellular pH (Barnes & Bui, 1990; Mahmud & Barnes, 1992). Attwell *et al.* (1987) described a synaptic transfer function relating postsynaptic horizontal cell voltage to presynaptic rod voltage (see Figure 19A). This synaptic transfer function can be modified and represented as current. If this function is then shifted along the

voltage axis by the amounts prescribed by the pH dependent shifts in Ca channel activation, the results in Figure 16 can be accounted for.

4.2.3 Activity Dependent pH Changes Are Widespread In The Nervous System

Activity dependent pH changes have been described for a variety of preparations including cerebellum, cortex, hippocampus, spinal cord, nerve and retina (see reviews by Chesler, 1990, and Chesler & Kaila, 1992). Specifically, light-induced changes have been recorded to be 0.2 pH unit in minutes in cat (Yamamoto, Borgula, & Steinberg, 1992), 0.02 pH unit in toad (Oakley, II. & Wen, 1989), and with prolonged illumination, 0.07 pH unit in frog (Borgula, Karwoski, & Steinberg, 1989). Winkler (1981) showed that lactic acid production from the rat retina increased in the dark. Furthermore, aerobic lactic acid production was decreased by about 10 % when the retina was exposed to 30 minutes of light. Linsenmeier (1986) made measurements of oxygen tension and voltage with double-barreled oxygen microelectrodes. He found that oxygen consumption decreased about 50 % when the cat retina was exposed to 60 s of rod saturating illumination. Changes were maximal in the outer nuclear layer. This suggests that the retina is probably metabolically active in the dark. In the light, oxygen consumption is reduced and lactic acid production is slightly decreased.

4.2.4 Relevance To Synaptic Gain

pH modulation of synaptic transfer is a novel mechanism of regulation of a synapse. It may serve as an adaptive mechanism by which under light-adapted conditions in the retina, the gain of the synapse would be increased. In the dark, photoreceptors are metabolically active and are producing and extruding lactic acid (see above). Extracellular pH may therefore be more acidic. The photoreceptor synapse however is still very active. Light hyperpolarizes the photoreceptor and shuts off synaptic transmission. Light also reduces metabolic activity by about

10 %. In the range of pH_O 7 to 8 this might be a change from pH_O 7.6 to pH_O 7.7. This would tend to increase Ca channel activity and turn up the gain of the synapse. The cell would then be working under a different synaptic transfer function.

Activity dependent pH_O transients in the retina described elsewhere could alter synaptic transmission by resetting the synaptic transfer function of the synapse. In addition, such modification of could play a role in clinical aspects of hypoxia where there is an initial increase in glycolysis and lactic acid production (Lutz, 1992). This may serve, at least initially, as a protective mechanism by reducing Ca entry into the cell and reducing cytotoxicity.

If presynaptic Ca channels underlie the synaptic transfer function in other neurons, and they have the same pH-sensitivity of those in photoreceptors, proton regulation of transmission via this mechanism could be an important feature of CNS function.

4.3 Mechanisms Of Feedback

Several mechanisms have been proposed to account for surround illumination evoked depolarization of cones and for the generation of center-surround receptive fields in second order cells. They include feed-forward synaptic transmission from horizontal cells to bipolar cells (for which anatomical evidence exists), synaptic feedback from horizontal cells to cones (for which electrophysiological evidence exists) and electric field potentials in the photoreceptor-horizontal cell extracellular gap. Synaptic feedback from horizontal cells to cones has been investigated here.

4.3.1 The Feedback Response Reversal Potential Varies

The feedback response was best observed using the headless cone technique described by Attwell *et al.* (1983). Here broad field illumination served as the perfect annulus for a headless cone to generate synaptically driven responses. A cone held at a potential of -60 mV had a feedback signal that was 40 pA in amplitude. Holding the cell at more depolarized potentials reduced the amplitude of the feedback signal. It was determined through extrapolation of the peak of the feedback signal that it reversed near 0 mV.

Studies on surround evoked prolonged depolarizations in cones have suggested that the chloride equilibrium potential (E_{Cl}) in cones is more positive than the dark potential (-40 mV; Thoreson & Burkhardt, 1990; Lasansky, 1981). This may be the case with the data shown in Figure 21 in which a Na-K pipette solution with 107 mM Cl^- was used. E_{Cl} in this cell may be artificially elevated to near 0 mV. It is possible that the use of KCl microelectrodes by Thoreson and Burkhardt (1990) and Lasansky (1981) may have elevated E_{Cl} artificially such that the feedback response was depolarizing in direction. However, similar experiments

carried out with K Acetate (which shouldn't elevate E_{Cl}) electrodes gave similar depolarizing feedback responses (Thoreson & Burkhardt, 1990; Lasansky, 1981).

Wu (1992) recorded the feedback signal from tiger salamander cones that had their outer segments truncated. The reversal potential of the feedback signal and therefore, E_{Cl} was measured to be -67 mV. Skryzpek and Werblin (1983) also determined that E_{Cl} is negative to the dark potential. These experiments were carried out using microelectrodes filled with K Acetate which should prevent artificial elevation of E_{Cl} .

It is still not clear what the chloride equilibrium potential is. Further experiments need to be carried out shifting E_{Cl} to determine the effects on the feedback response.

4.3.2 GABA May Modulate Calcium-Activated Currents

Figures 22 and 23 show that calcium-activated currents of cones may be modulated by GABA and may suggest a role for $GABA_B$ (Barnes & Hille, 1989) or $GABA_C$ (Matthews, Ayoub, & Heidelberger, 1991) receptors in feedback. The irreversibility of the GABA effect could be due to a peculiar, sudden rundown of calcium channel activity or due to dialysis and washout of a second messenger. However, $I_{Cl}(Ca)$ in normal bath solution is not greatly reduced with prolonged recordings suggesting that Ca channels under normal recording conditions do not significantly rundown. This suggests that GABA may be modulating Ca channels of cone photoreceptors via $GABA_B$ or $GABA_C$ receptors.

Feedback to salamander cones in slices have been shown to be blocked by 100 μ M bicuculline (Wu, 1991) while baclofen and phaclofen ($GABA_B$ receptor analogues) had no effect. It is likely that GABA released from horizontal cells onto cone photoreceptors acts via $GABA_A$ receptors as proposed for turtle (Tachibana & Kaneko, 1984; Kaneko & Tachibana, 1986). Interestingly, Thoreson &

Burkhardt (1990) found that various GABA agonists and antagonists had no effect on the surround-evoked depolarizations thought to be the feedback response in turtle cones. As is the case for the chloride equilibrium potential, the nature of the receptors involved in feedback to cones remains to be resolved.

4.4 Function Of The OPL

The outer plexiform layer of the vertebrate retina is the site of lateral interaction and early processing of visual information. It serves to generate center-surround antagonistic receptive fields for horizontal cells and bipolar cells.

4.4.1 Contrast Enhancement

How does this layer enhance contrast or detect edges? First of all, consider broad field illumination (i.e. no edges) falling on a perfectly concentric antagonistic receptive field. Central and surround cones are stimulated equally and the entire bipolar cell receptive field is stimulated. Lateral inhibition essentially cancels central and surround responses and the bipolar cell responds minimally. An edge (a light and dark area) that cuts through exactly one half of the bipolar cell receptive field will also produce a minimal response in the bipolar cell. Once again, responses of cones in one half of the bipolar cell receptive field are cancelled out by lateral inhibitory responses of cones in one half of the bipolar cell antagonistic surround. However, an edge transecting more than half of the bipolar cell receptive field will produce a greater response in the bipolar cell. Responses of cones in the central region of the bipolar cell receptive field will outweigh responses of cones in the antagonistic surround region. The bipolar cell response will be greater because of unbalanced weighting of responses in central and surround regions and this comprises an "edge" signal that will be transmitted to proximal levels of the retina and to the central nervous system.

The analysis of input-output relations of cones focused on the photoreceptor output synapse and feedback to cones. The photoreceptor output synapse is the direct path of information flow to second order cells. Activity dependent pH_O changes shift the synaptic transfer characteristics of the synapse by affecting gain, reliability and stability. Its action will further determine how inputs from horizontal

cells reach the photoreceptors. Thus changes of pH_O may also affect feedback to cones.

4.4.2 Outputs and Inputs in the OPL

Suppose a cone is resting at a dark potential of -40 mV and pH_O is 7.60. It is continuously releasing its transmitter glutamate onto horizontal cells that are then maintained at a depolarized potential near -30 mV. The horizontal cell is therefore continuously releasing its transmitter, presumably GABA, onto cones. If E_{Cl} is negative to the cone dark potential, then the effect of GABA would probably oppose the depolarizing influences of currents from the outer and inner segments. A balance is reached to maintain cone dark potential at -40 mV. Light (broad field) will hyperpolarize the cone, reduce glutamate release and hyperpolarize the horizontal cell. Horizontal cell GABA release will reduce and the GABA receptor mediated conductance in cones will decrease resulting in cell depolarization.

With prolonged illumination, it is expected that pH_O will alkalinize and shift cone Ca channel activation negative in the photoreceptor operating range. Light-induced hyperpolarization of the cone would be opposed by the activation of Ca channels at this negative range. As such, the cone would become more sensitive to changes in light level. This change in sensitivity or adaptation would then be reflected at the output synapse and consequently at the feedback synapse.

pH modulation of synaptic transmission in the outer plexiform layer may have clinical implications for hypoxia. Ca channels in other regions of the central nervous system may also exhibit a pH_O sensitivity suggesting that pH_O may serve as an extensive neuromodulator. Furthermore, it will be interesting to compare this cone model to synaptic interactions in local (nonspiking) circuits more generally in the nervous system.

References

- Attwell, D., Borges, S., Wu, S.M., & Wilson, M. (1987). Signal clipping by the rod output synapse, Nature, 328, 522-524.
- Attwell, D., Werblin, F.S., & Wilson, M. (1982). The properties of single cones isolated from the tiger salamander retina, Journal of Physiology (London), 328, 259-283.
- Attwell, D., Werblin, F.S., Wilson, M., & Wu, S.M. (1983). A sign-reversing pathway from rods to double and single cones in the retina of the tiger salamander, Journal of Physiology, 330, 313-333.
- Attwell, D., Wilson, M., & Wu, S. (1984). A quantitative analysis of interactions between photoreceptors in the salamander (*Ambystoma*) retina, Journal of Physiology (London), 352, 703-737.
- Ayoub, G.S. & Lam, D.M.-K. (1984). The release of γ -aminobutyric acid from horizontal cells of the goldfish (*Carassius auratus*) retina, Journal of Physiology, 355, 191-214.
- Bader, C.R. & Bertrand, D. (1984). Effect of changes in intra- and extracellular sodium on the inward (anomalous) rectification in salamander photoreceptors, Journal of Physiology, 347, 611-631.
- Barnes, S. & Bui, Q. (1991). Modulation of calcium-activated chloride current via pH-induced changes of calcium channel properties in cone photoreceptors, The Journal of Neuroscience, 11, 4015-4023.
- Barnes, S. & Hille, B. (1989). Ionic channels of the inner segment of tiger salamander cone photoreceptors, Journal of General Physiology, 94, 719-743.
- Barnes, S., Merchant, V., & Mahmud, F. Presynaptic modulation of transmission gain by protons at the photoreceptor output synapse. (Submitted).
- Baylor, D.A., Fuortes, M.G.F., & O'Bryan, P.M. (1971). Receptive fields of single cones in the retina of the turtle, Journal of Physiology, 214, 256-294.
- Beech, D. & Barnes, S. (1989). Characterization of a voltage-gated K⁺ channel that accelerates the rod response to dim light, Neuron, 3, 573-581.
- Bitensky, M.W., Wheeler, G.L., Yamazaki, A., Rasenick, M.M., & Stein, P.J. (1981). Cyclic-nucleotide metabolism in vertebrate photoreceptors: A remarkable analogy and an unraveling enigma, in Molecular mechanisms of photoreceptor transduction, W.H. Miller, ed., Current Topics in Membrane Transport, 15, 238-272.
- Borgula, G.A., Karwoski, C.J., & Steinberg, R.H. (1989). Light-evoked changes in extracellular pH in frog retina, Brain Research, 29, 1069-1077.

- Byzov, A.L. & Shura-Bura, T.M. (1986). Electrical feedback mechanism in the processing of signals in the outer plexiform layer of the retina, Brain Research, 26, 33-44.
- Byzov, A.L., Golubtzov, K.V., & Trifonov, Ju.A. (1977). The model of mechanism of feedback between horizontal cells and photoreceptors in vertebrate retina, in Vertebrate Photoreception, H.B. Barlow & P. Fatt, eds.: New York.
- Cervetto, L. & MacNichol, Jr. E.F. (1972). Inactivation of horizontal cells in turtle retina by glutamate and aspartate, Science, 178, 767-768.
- Chesler, M. & Kaila, K. (1992). Modulation of pH by neuronal activity, Trends in Neuroscience, 15, 396-402.
- Chesler, M. (1990). The regulation and modulation of pH in the nervous system, Progress in Neurobiology, 34, 401-427.
- Christensen, B.N. & Hida, E. (1990). Protonation of histidine groups inhibits gating of the quisqualate/kainate channel protein in isolated catfish cone horizontal cells, Neuron, 5, 471-478.
- Copenhagen, D.R., Ashmore, J.F., & Schnapf, J.K. (1983). Kinetics of synaptic transmission from photoreceptors to horizontal and bipolar cells in turtle retina, Vision Research, 23, 363-369.
- Dartnall, H.J.A. (1958). The interpretation of spectral sensitivity curves, British Medical Bulletin, 9, 24-30.
- Dowling, J.E. & Ripps, H. (1972). Adaptation in skate photoreceptors, Journal of General Physiology, 60, 698-719.
- Dowling, J.E. & Werblin, F.S. (1969). Organization of retina of the mudpuppy, *Necturus maculosus*. I. Synaptic structure, Journal of Neurophysiology, 32, 315-338.
- Dowling, J.E. (1968). Synaptic organization of the frog retina: an electron microscopic analysis comparing the retinas of frogs and primates, Proceedings of the Royal Society of London, Series B, 170, 205-228.
- Dowling, J.E. (1987). The Retina: An approachable part of the brain. Belknap Press of Harvard University Press: Cambridge, Massachusetts.
- Fain, G. & Dowling, J.E. (1973). Intracellular recordings from single rods and cones in the mudpuppy retina, Science, 180, 1178-1181.
- Fesenko, E.E., Kolenikov, S.S., & Lyuborsky, A.L. (1985). Induction by cyclic GMP of cationic conductance plasma membrane of retinal rod outer segment, Nature, 313, 310-313.

- Harsanyi, K. & Mangel, S.C. (1992). Modulation of cone to horizontal cell transmission by calcium and pH in the fish retina, Visual Neuroscience, in press.
- Haynes, L. & Yau, K.-W. (1985). Cyclic GMP-sensitive conductance in outer segment membrane of catfish cones, Nature, 317, 61-64.
- Hille, B. (1992). Ionic Channels of Excitable Membranes. 2nd Edition, Sinauer Associates Inc.: Sunderland, Massachusetts.
- Hodgkin, A.L. & Huxley, A.F. (1952). A quantitative description of membrane current and its application to conduction and excitation in nerve, Journal of Physiology (London), 117, 500-544.
- Hodgkin, A.L. & Nunn, B.J. (1987). The effect of ions and sodium-calcium exchange in salamander rods, Journal of Physiology (London), 391, 371-398.
- Ishida, A.T. & Fain, G.L. (1981). d-Aspartate potentiates the effect of l-glutamate on horizontal cells in goldfish retina, Proceedings of the National Academy of Science, U.S.A., 78, 5890-5894.
- Johnston, D. & Lam, D.M.-K. (1981). Regenerative and passive membrane properties of isolated horizontal cells from a teleost retina, Nature, 292, 451-454.
- Kaneko, A. & Tachibana, M. (1986). Effects of γ -aminobutyric acid on isolated cone photoreceptors of the turtle retina, Journal of Physiology (London), 373, 443-461.
- Kleinschmidt, J. (1991). Signal transmission at the photoreceptor synapse. Role of calcium ions and protons, Annals of the New York Academy of Science, 635, 468-470.
- Kolb, H. & Jones, J. (1984). Synaptic organization of the outer plexiform layer of the turtle retina: An electron microscope study of serial sections, Journal of Neurocytology, 13, 567-591.
- Kraft, T.W. & Burkhardt, D.A. (1986). Telodendrites of cone photoreceptors: Structure and probable function, The Journal of Comparative Neurology, 249, 13-27.
- Kuffler, S. (1953). Discharge patterns and functional organization of mammalian retina, Journal of Neurophysiology, 16, 37-68.
- Kuffler, S.W., Nicholls, J.G., & Martin, A.R. (1984). From Neuron to Brain: A Cellular Approach to the Function of the Nervous System, 2nd Edition, Sinauer Associates, Inc.: Sunderland, Massachusetts.
- Lasansky, A. (1969). Basal junctions at synaptic endings of turtle visual cells, Journal of Cell Biology, 40, 577-581.

- Lasansky, A. (1971). Synaptic organization of cone cells in the turtle retina. Philosophical Transactions of the Royal Society of London, Series B, Biological Sciences, 262, 365-381.
- Lasansky, A. (1973). Organization of the outer synaptic layer in the retina of the larval tiger salamander, Philosophical Transactions of the Royal Society of London, Series B, 265, 471-489.
- Lasansky, A. (1978). Contacts between receptors and electrophysiologically identified neurones in the retina of the tiger salamander. Journal of Physiology, 285, 531-542.
- Lasansky, A. (1981). Synaptic action mediating cone responses to annular illumination in the retina of the larval tiger salamander, Journal of Physiology, 310, 205-214.
- Lasater, E.M. & Dowling, J.E. (1982). Carp horizontal cells in culture respond selectively to l-glutamate and its antagonists, Proceedings of the National Academy of Science, U.S.A., 79, 936-940.
- Lasater, E.M., Dowling, J.E., & Ripps, H. (1984). Pharmacological properties of isolated horizontal and bipolar cells from the skate retina, The Journal of Neuroscience, 4, 1966-1975.
- Lasater, E.M. & Witkovsky, P. (1991). The calcium current of turtle cone photoreceptor axon terminals, Neuroscience Research, Supplement, 15, S165-S173.
- Liebman, P.A., Mueller, P., & Pugh, Jr., E.N. (1984). Protons suppress the dark current of frog retinal rods, Journal of Physiology (London), 347, 85-110.
- Liebman, P.A. & Pugh, Jr. E.N. (1981). Control of rod disk membrane phosphodiesterase and a model for visual transduction, in Molecular mechanisms of photoreceptor transduction, W.H. Miller, ed., Current Topics in Membrane Transport, 15, 157-171.
- Linsenmeier, R.A. (1986). Effects of light and darkness on oxygen distribution and consumption in the cat retina, The Journal of General Physiology, 88, 521-542.
- Lutz, P.L. (1992). Mechanisms for anoxic survival in the vertebrate retina, Annual Review of Physiology, 54, 601-618.
- Mahmud, F. & Barnes, S. (1992). Modulation of Ca channel properties by extracellular pH in rod photoreceptors, Society for Neuroscience Abstracts, 18, 837.
- Marc, R.E., Stell, W.K., Bok, D., & Lam, D.M.-K. (1978). GABA-ergic pathways in the goldfish retina, The Journal of Comparative Neurology, 182, 221-246.

- Marshak, D.W. & Dowling, J.E. (1987). Synapses of cone horizontal cell axons in goldfish retina, Journal of Comparative Neurology, 256, 430-443.
- Matthews, G., Ayoub, G., & Heidelberger, R. (1991). Inhibition of presynaptic calcium current via GABA_C receptors, Society for Neuroscience Abstracts, 17, 900.
- Matthews, G. & Baylor, D.A. (1981). The photocurrent and dark current of retinal rods, in Molecular mechanisms of photoreceptor transduction, W.H. Miller, ed., Current Topics in Membrane Transport, 15, 4-18.
- Merchant, V. & Barnes, S. (1991). Lateral signal propagation via cone telodendrites in tiger salamander retina, Society for Neuroscience Abstracts, 17, 298.
- Merchant, V. & Barnes, S. (1992). Modulation of synaptic transfer by extracellular pH at the photoreceptor output synapse, Society for Neuroscience Abstracts, 18, 837.
- Miller, W.H. (1981). Ca²⁺ and cGMP, in Molecular mechanisms of photoreceptor transduction, W.H. Miller, ed., Current Topics in Membrane Transport, 15, 441-445.
- Murakami, M., Ohtsu, K., & Ohtsuka, T. (1972). Effects of chemicals on receptors and horizontal cells in the retina, Journal of Physiology, 227, 899-913.
- Murakami, M., Shimoda, Y., Nakatani, K., Miyachi, E., & Watanabe, S. (1982a). GABA-mediated negative feedback and color opponency in carp retina. Japanese Journal of Physiology, 32, 927-935.
- Murakami, M., Shimoda, Y., Nakatani, K., Miyachi, E., & Watanabe, S. (1982b). GABA-mediated negative feedback from horizontal cells to cones in carp retina, Japanese Journal of Physiology, 32, 911-926.
- Nakatani, K. & Yau, K.-W. (1985). cGMP opens the light-sensitive conductance in retinal rods, Biophysical Journal, 47, 356a.
- Nawy, S. & Jahr, C.E. (1990). Suppression by glutamate of cGMP-activated conductance in retinal bipolar cells. Nature, 346, 269-271.
- Nawy, S. & Jahr, C.E. (1991). cGMP-gated conductance in retinal bipolar cells is suppressed by the photoreceptor transmitter, Neuron, 7, 677-683.
- Negishi, K., Teranishi, T., & Kato, S. (1985). Opposite effects of ammonia and carbon dioxide on dye coupling between horizontal cells in the carp retina, Brain Research, 342, 330-339.
- Nowycky, M.C., Fox, A.P., & Tsien, R.W. (1985). Three types of neuronal calcium channels with different calcium agonist sensitivity, Nature, 316, 440-443.

- Oakley, II, B. & Wen, R. (1989). Extracellular pH in the isolated retina of the toad in darkness and during illumination, Journal of Physiology (London), 419, 353-378.
- Perkel, D.H. & Mulloney, B. (1978). Electrotonic properties of neurons: Steady-state compartmental model, Journal of Neurophysiology, 41, 621-639.
- Sakai, H.M. & Naka, K.-I. (1986). Synaptic organization of the cone horizontal cells in the catfish retina, The Journal of Comparative Neurology, 245, 107-115.
- Schnapf, J.L. & McBurney, R.N. (1980). Light-induced changes in membrane current in cone outer segments of tiger salamander and turtle, Nature, 287, 239-241.
- Shiells, R.A. & Falk, G. (1992a). The glutamate-receptor linked cGMP cascade of retinal on-bipolar cells is pertussis and cholera toxin-sensitive, Proceedings of the Royal Society of London, Series B, 247, 17-20.
- Shiells, R.A. & Falk, G. (1992b). Properties of the cGMP-activated channel of retinal on-bipolar cells, Proceedings of the Royal Society of London, Series B, 247, 21-25.
- Sillman, A.J., Owen, W.G., & Fernandez, H.R. (1972). The generation of the late receptor potential: An excitation-inhibition phenomenon, Vision Research, 12, 1519-1531.
- Skrzypek, J. & Werblin, F. (1983). Lateral interactions in absence of feedback to cones, Journal of Neurophysiology, 49, 1007-1016.
- Slaughter, M.M. & Miller, R.F. (1981). 2-Amino-4-Phosphonobutyric acid: A new pharmacological tool for retina research, Science, 211, 182-185.
- Slaughter, M.M. & Miller, R.F. (1983a). An excitatory amino acid antagonist blocks cone input to sign-conserving second-order retinal neurons, Science, 219, 1230-1232.
- Slaughter, M.M. & Miller, R.F. (1985). Identification of a distinct synaptic glutamate receptor on horizontal cells in mudpuppy retina, Nature, 314, 96-97.
- Spray, D.C., Harris, A.L., & Bennett, M.V.L. (1981). Gap junctional conductance is a simple and sensitive functions of intracellular pH, Science, 211, 712-715.
- Stell, W.K., & Lightfoot, D.O. (1975). Color-specific interconnections of cones and horizontal cells in the retina of the goldfish, Journal of Comparative Neurology, 159, 473-502.
- Stewart, W.W. (1978). Functional connections between cells as revealed by dye-coupling with a highly fluorescent naphthalimide tracer, Cell, 14, 741-759.

- Stryer, L. (1986). Cyclic GMP cascade of vision, Annual Review of Neuroscience, 9, 87-119.
- Stryer, L., Hurley, J.B., & Fung, B.K.-K. (1981). First stage of amplification in the cyclic-nucleotide cascade of vision, in Molecular mechanisms of photoreceptor transduction, W.H. Miller, ed., Current Topics in Membrane Transport, 15, 93-108.
- Sullivan, J.M. & Lasater, E.M. (1992). Sustained and transient calcium currents in horizontal cells of the white bass retina, Journal of General Physiology, 99, 85-107.
- Tachibana, M. & Kaneko, A. (1984). γ -Aminobutyric acid acts at axon terminals of turtle photoreceptors: Difference in sensitivity among cell types, Proceedings of the National Academy of Science, U.S.A., 81, 7961-7964.
- Tang, C.-M., Dichter, M., & Morad, M. (1990). Modulation of the N-methyl-D-aspartate channel by extracellular H^+ , Proceedings of the National Academy of Science, U.S.A., 87, 6445-6449.
- Thoreson, W.B. & Burkhardt, D.A. (1990). Effects of synaptic blocking agents on the depolarizing responses of turtle cones evoked by surround illumination, Visual Neuroscience, 5, 571-583.
- Traynelis, S.F. & Cull-Candy, S.G. (1990). Proton inhibition of N-methyl-D-aspartate receptors in cerebellar neurons, Nature, 345, 347-350.
- Ueda, Y., Kaneko, A., & Kaneda, M. (1992). Voltage-dependent ionic currents in solitary horizontal cells isolated from cat retina, Journal of Neurophysiology, 68, 1143-1150.
- Walls, G.L. (1942). The Vertebrate Eye and Its Adaptive Radiation. Cranbrook Institute of Science: Bloomfield, Michigan.
- Werblin, F.S. & Dowling, J.E. (1969). Organization of the retina of the mudpuppy, *Necturus maculosus*. II. Intracellular recording, Journal of Neurophysiology, 32, 339-355.
- Werblin, F.S. (1978). Transmission along and between rods in the tiger salamander retina, Journal of Physiology, 280, 449-470.
- Wilson, M., Gleason, E., & Gilbertson, T. (1991). The transmission of signals from photoreceptors to postsynaptic cells in the vertebrate retina, Neuroscience Research, Supplement, 15, S25-S39.
- Winkler, B.S. (1981). Glycolytic and oxidative metabolism in relation to retinal function, The Journal of General Physiology, 77, 667-692.
- Wu, S.M. & Dowling, J.E. (1978). l-Aspartate: Evidence for a role in cone photoreceptor synaptic transmission in the carp retina, Proceedings of the National Academy of Science, U.S.A., 75, 5205-5209.

- Wu, S.M. & Yang, X.-L. (1988). Electrical coupling between rods and cones in tiger salamander retina, Proceedings of the National Academy of Science, U.S.A., 85, 275-278.
- Wu, S.M. (1986). Effects of gamma-amino butyric acid on cone and bipolar cells of the tiger salamander retina, Brain Research, 365, 70-77.
- Wu, S.M. (1991). Input-output relations of the feedback synapse between horizontal cells and cones in the tiger salamander retina, Journal of Neurophysiology, 65, 1197-1206.
- Yamamoto, F., Borgula, G.A., & Steinberg, R.H. (1992). Effects of light and darkness on pH outside rod photoreceptors in the cat retina, Experimental Eye Research, 54, 689-697.
- Yang, X.-L. & Wu, S.M. (1991). Coexistence and function of glutamate receptor subtypes in the horizontal cells of the tiger salamander retina, Visual Neuroscience, 7, 377-382.
- Yazulla, S. (1985). Evoked efflux of [³H] GABA from goldfish retina in the dark, Brain Research, 325, 171-180.